Received: 1 October 2018 | Revised: 21 January 2019 | Accepted: 22 January 2019

DOI: 10.1002/jnr.24396

RESEARCH ARTICLE

GABA-containing compound gammapyrone protects against brain impairments in Alzheimer's disease model male rats and prevents mitochondrial dysfunction in cell culture

Vladimirs Pilipenko[1] | Karina Narbute[1] | Ines Amara[2] | Angela Trovato[2] | Maria Scuto[2] | Jolanta Pupure[1] | Baiba Jansone[1] | Janis Poikans[3] | Egils Bisenieks[3] | Vija Klusa[1] | Vittorio Calabrese[2]

[1]Faculty of Medicine, Department of Pharmacology, University of Latvia, Riga, Latvia

[2]Department of Biomedical and Biotechnological Sciences, University of Catania, Italy

[3]Laboratory of Membrane Active Compounds, Latvian Institute of Organic Synthesis, Riga, Latvia

Correspondence
Vladimirs Pilipenko, Department of Pharmacology, Faculty of Medicine, University of Latvia, 1 Jelgavas St., LV-1004, Riga, Latvia.
Email: vladimirs.pilipenko@lu.lv

Abstract

Neuroinflammation, oxidative stress, decreased glucose/energy metabolism, and disrupted neurotransmission are changes that occur early in sporadic Alzheimer's disease (AD), manifesting as mild cognitive impairment. Recently, the imbalanced function of the gamma-aminobutyric acid (GABA) system was identified as a critical factor in AD progression. Thus, maintaining balance among neurotransmitter systems, particularly the GABA system, can be considered a beneficial strategy to slow AD progression. The present study investigated the effects of the compound gammapyrone, a molecule containing three GABA moieties: "free" moiety attached to the position 4 of the 1,4-dihydropyridine (DHP) ring, and two "crypto" moieties as part of the DHP scaffold. The "free" and "crypto" GABA moieties are linked by a peptide bond (–CONH–), resulting in a peptide-mimicking structure. In a nontransgenic male rat AD model generated by intracerebroventricular (icv) streptozocin (STZ) administration, gammapyrone (0.1 and 0.5 mg/kg ip) mitigated the impairment of spatial learning and memory, prevented astroglial and microglial neuroinflammation, and normalized acetylcholine breakdown and GABA biosynthesis. In PC12 cells, gammapyrone protected against oxidative stress, mitochondrial dysfunction and apoptosis caused by the mitochondrial toxin di-2-ethylhexyl phthalate (DEHP). Gammapyrone did not bind to GABA-A and GABA-B receptors in vitro; therefore, we cannot attribute its neuroprotective action to a specific interaction with GABA receptors. Nevertheless, we suggest that the peptide-like regulatory mechanisms of gammapyrone or its allosteric modulatory properties are essential for the observed effects. Since, the icv STZ model resembles the early stages of AD, gammapyrone, and/or its congeners could be useful in the design of anti-dementia drugs.

KEYWORDS

bioenergetics, GABA, intracerebroventricular streptozocin, PC12 cells, protein expression, spatial learning/memory

Significance

In this study, rat model of intracerebroventricular streptozocin injection was used to resemble sporadic Alzheimer's disease (AD). We demonstrated that gammapyrone, a compound that contains three gamma-aminobutyric acid moieties in its structure, possesses memory-enhancing, anti-inflammatory and neurotransmitter regulating activities in vivo and protects against oxidative stress, apoptosis and mitochondrial dysfunction in vitro. These properties indicate the ability of gammapyrone to target the early changes that occur before amyloidosis. Gammapyrone and/or its congeners could be useful in the design of novel disease-modifying drugs for the prevention of cognitive decline in predementia AD stages.

1 | INTRODUCTION

Alzheimer's disease (AD) is a multifaceted, progressive neurodegenerative disease that includes several detrimental processes in the brain: neuroinflammation (Calsolaro & Edison, 2016; Pennisi et al., 2017); neurotransmitter system dysregulation (Correia, Perry, & Moreira, 2016); increased oxidative stress (Calabrese et al., 2018; Pennisi et al., 2017) and glucose and energy metabolism dysfunction (Abolhassani et al., 2017; Duran-Aniotz & Hetz, 2016). All of these impairments result in the accumulation of amyloid-beta (Aβ) and other misfolded proteins (Lithfous, Dufour, & Després, 2013). Promising strategies to combat AD consist of early interventions and disease-modifying approaches that can be implemented before the formation of Aβ plaques and amyloidosis (Liu, Chen et al., 2018). Thus, a search for novel cellular targets and therapies should aim to stop AD before it develops (McDade & Bateman, 2017) and shift the strategy from the treatment of late-stage pathology to early stage pathophysiology (Styr and Slutsky, 2018). One such approach could be targeting the gamma-aminobutyric acid ([GABA]ergic) system, since this system is able to stabilize the intracellular processes that are impaired in AD (Nava-Mesa, Jiménez-Díaz, Yajeya, & Navarro-Lopez, 2014).

In this context, our question was whether a compound that contains GABA moieties would have a role in neuroregulation and restore cellular homeostasis. In this regard, we studied gammapyrone, a compound with three GABA moieties: one natural or "free" moiety attached to position 4 of the 1,4-dihydropyridine (DHP) ring, and two "crypto" GABA moieties as part of DHP scaffold moieties (Figure 1). The "free" and "crypto" GABAs are linked by a peptide bond (–CONH–), and thus resemble a peptidomimetic structure (Klusa, 2016). However, we cannot ignore the fact that there is a double bond (–C=C–) between atoms 2 and 3 and between atoms 5 and 6 of the "crypto" GABA moieties in the DHP ring; thus, the "crypto" GABA moieties can be described as unsaturated amino acids. Unsaturated amino acids are potential precursors to the cross-linkages in peptides and proteins (Gross, 1977).

Previously, DHP compounds that contained other "free" amino acids, for example, glutamate-containing glutapyrone (Misane et al., 1998) and taurine-containing tauropyrone (Dzirkale et al., 2011) have shown different activities in animal models. Additionally, amino-acid containing DHPs differed quantitatively and qualitatively from typical DHP agents (mostly antihypertensive drugs) by their high solubility, lack of calcium antagonism and antihypertensive properties, as well as very low toxicity and neuromodulatory/regulatory efficacy at low doses (for review see Klusa, 2016).

In this study, we assessed for the first time the influence of gammapyrone in the male rat streptozocin (STZ)-induced nontransgenic AD model. A crucial difference between the STZ model and the more frequently used transgenic AD models is that the former mimics sporadic AD that constitutes 95% of all AD cases, whereas

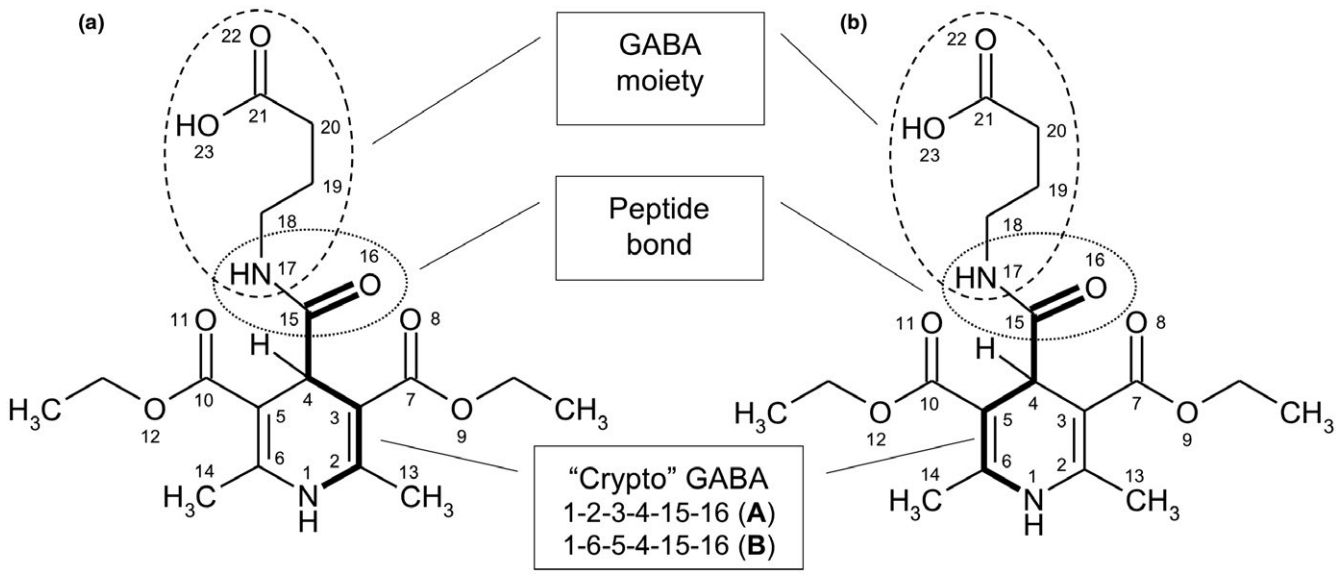

FIGURE 1 Structure of gammapyrone: natural GABA moiety or "free" GABA (17–18–19–20–21–22–23) and "crypto" GABAs (a: 1–2-3–4-15–16 and b: 1–6-5–4-15–16)

transgenic models resemble the familial form of AD that constitutes only 5% of all AD cases (Grieb, 2016). STZ model mimics the early behavioral, neuropathological, and metabolical features of sporadic AD that share similarities with sporadic AD in humans (Salkovic-Petrisic, Knezovic, Hoyer, & Riederer, 2013). These features include impairments in brain glucose metabolism (De la Monte & Wands, 2008), neuroinflammation (Rai, Kamat, Nath, & Shukla, 2014), oxidative stress (Tiwari, Kuhad, Bishnoi, & Chopra, 2009), as well as brain mitochondrial abnormalities (Saxena, Patro, & Nath, 2011). These changes precede and eventually lead to tau and amyloid-beta pathologies and are interdependent with pathological changes in the epigenetic mechanisms, namely: (a) aberrations of DNA methylation, (b) histone deacetylation and subsequent chromatin remodeling, and (c) dysregulation of noncoding RNAs (Liu, Jiao, & Shen, 2018).

STZ model, therefore, represents a valid experimental tool to obtain new insights regarding both early and late brain changes which can be translated in novel approaches in the treatment of this disease.

We assessed spatial learning/memory with the Morris water maze test and of locomotor activity with the open field test. Ex vivo, we determined the expression of cortical and hippocampal proteins related to neuroinflammation (glial fibrillary acidic protein, GFAP; ionized calcium-binding adapter molecule-1, Iba-1), synthesis of GABA (glutamic acid decarboxylase 67, GAD67), and degradation of acetylcholine (AChE). In vitro, binding assays were performed for GABA-A and GABA-B receptors. Neuronal PC12 cells were treated with mitochondrial toxin di-2-ethylhexyl phthalate (DEHP), and the effects of gammapyrone on DEHP-induced oxidative stress and mitochondrial dysfunction were also determined.

2 | MATERIALS AND METHODS

2.1 | Animals

Male Wistar rats (280 ± 20 g, 9 weeks old) were obtained from the Laboratory Animal Center, University of Tartu, Estonia. In the STZ model of sporadic AD, sex differences exist; it has been reported that learning/memory impairments and several other pathological events of AD that were observed in male rats were not observed in female rats (Bao et al., 2017). All efforts were made to minimize animal suffering and to reduce the number of animals used. The experiments were conducted in accordance with the EU Directive 2010/63/EU and local laws and policies on the protection of animals used for scientific purposes. The animal protocol for this study was approved by the Animal Ethics Committee of the Food and Veterinary Service, Riga, Latvia. The animals were housed in polypropylene cages (five rats per cage) with food (R70, Lantmännen, Sweden) and water provided ad libitum, and kept in a controlled laboratory environment (temperature 22 ± 2°C, humidity 50–60%, 12/12 hr light/dark cycle).

2.2 | Chemicals and antibodies

Gammapyrone was synthesized in the Laboratory of Membrane Active Compounds of the Latvian Institute of Organic Synthesis (Riga, Latvia). Artificial cerebrospinal fluid (aCSF) was prepared ex tempore (mmol/L): 147 mM NaCl, 2.9 mM KCl, 1.6 mM $MgCl_2$, 1.7 mM $CaCl_2$ and 2.2 mM D-glucose were dissolved in water for injection. The following reagents were purchased from Sigma-Aldrich (USA): 3,3′-diaminobenzidine (DAB, D5905), anti-GAD67 antibody (sc28376), anti-GFAP antibody (G3893), di-2-ethylhexyl phthalate (DEHP, D201154), ethopropazine (E5406), ExtrAvidin Peroxidase Staining Kit (EXTRA2–1 KT), haematoxylin solution (MHS16), and streptozocin (S0130). S-acetylthiocholine iodide (A16802) was obtained from Alfa Aesar (USA). Copper sulfate (102790), potassium hexacyanoferrate III (104973), and sodium citrate (106448) were acquired from Merck Millipore (USA). 3-(4,5-Dimethyl-2-thiazolyl)-2,5-diphenyl-2H-tetrazolium bromide (MTT), Dulbecco's modified Eagle medium (DMEM), horse serum, fetal bovine serum (FBS), phosphate-buffered saline (PBS), trypsin-ethylenediaminetetraacetic acid, penicillin-streptomycin mixture and L-glutamine were from GIBCO-BCL (UK). 2,7-Dichlorofluorescein diacetate (DCF-DA) was supplied by Molecular Probes (France). The antibodies used in this study are summarized in Table 1.

TABLE 1 Primary antibodies used in the study

Antigen	Immunogen description	Host species, source, catalog no.	Concentration used
Anti-GAD67	Synthetic peptide raised against amino acids 1-101 of GAD67 of human origin	Mouse monoclonal, Santa Cruz Biotechnology, sc-28376	1:500
Anti-GFAP	Generated against purified GFAP from pig spinal cord	Mouse monoclonal, Sigma-Aldrich, G3893	1:1000
Anti-Iba-1	Synthetic peptide raised against C-terminus of Iba-1	Rabbit polyclonal, Wako, 019-19741	1:2000
Anti-Bax	Raised against amino acids 1-171 of Baxα of mouse origin.	Mouse monoclonal, Santa Cruz Biotechnology, sc-7480, AB_626729	1:500
Anti-Bcl2	Raised against amino acids 1-205 of human Bcl-2	Santa Cruz Biotechnology, sc-7382	1:500
Anti-Caspase 3	Raised against amino acids 1-277 representing full length caspase-3 of human origin	Mouse monoclonal, Santa Cruz Biotechnology, sc-7272	1:500
Anti-p53	Raised against the synthetic phosphopeptide corresponding to residues surrounding serine 15 of human p53	Mouse monoclonal, Cell Signaling Technology, 9286	1:2000

2.3 | In vivo experiments

2.3.1 | Drug treatments

Animal group size was calculated based on preliminary study with a 5% two-sided significance level. To detect changes in spatial learning/memory performance, six groups (10 rats per group) were used, whereas to detect changes in biochemical outcomes, five rats were used per group. There were one control and five experimental groups. Depending on the group, the rats received intraperitoneal injections of either saline or gammapyrone once daily on experimental days 1–3 (prior to the icv injection of STZ or artificial cerebrospinal fluid [aCSF]) and once daily on experimental days 15–22 (Figure 2). This design was chosen to assess the prophylactic effects of gammapyrone on the STZ-induced changes. Behavioral tests on experimental days 18–22 were performed 30 min after the injections. The groups were the following: (a) saline ip and aCSF icv (Control); (b) saline ip and STZ icv; (c) gammapyrone 0.1 mg/kg ip and aCSF icv; (d) gammapyrone 0.1 + STZ icv; (e) gammapyrone 0.5 mg/kg ip and aCSF icv; (f) gammapyrone 0.5 mg/kg +STZ icv.

2.3.2 | Surgery

On experimental day 4, animals were anesthetized with isoflurane (3–3.5% for induction and 2% for maintenance) in N_2O and O_2 (70%/30% for induction and 50%/50% for maintenance). Animals were then fixed on a stereotaxic frame (Stoelting Inc., USA). The head was shaved and sterilized with an alcohol pad, and a sagittal incision in the midline was made. Two lateral holes were drilled in the skull in the two ventricles using the following coordinates (Paxinos & Watson, 2007): −0.7 mm anteroposterior, 1.7 mm mediolateral and −4.0 mm dorsoventral relative to bregma. Using Hamilton microsyringe, STZ was injected in these lateral ventricles (750 μg/10 μl in aCSF for each animal) at 1 μl/min and 5 μl per ventricle. Control group received bilateral injections of aCSF (5 μl/ventricle). For the diffusion of the substance, the microsyringe was left in place for 2 min after each infusion. A 14-day resting period was implemented for the development of cognitive deficiency. The exclusion criteria for the behavioral and biochemical tests were as follows: (a) changes in behavior (aggressiveness, changes in breathing (tachypnea/dyspnea), decrease in movement, abnormal gait, inability to be handled); (b) negative impact of environment (diarrhea with/without blood); and (c) worsening of visual appearance (unkempt coat, weight loss more than 20%).

Altogether, 11 animals were excluded from the experiments: 2 animals from the Control group, 3 animals from the STZ group, 1 animal from gammapyrone 0.1 + aCSF and gammapyrone 0.5 + aCSF groups and 2 animals from gammapyrone 0.1 + STZ and gammapyrone 0.5 + STZ groups.

2.3.3 | Open field test

To assess the changes in animal locomotor activity, we conducted an open field test on experimental day 18 (n = 8 in the control group, n = 7 in the STZ group, n = 9 in the gammapyrone 0.1 + aCSF and gammapyrone 0.5 + aCSF groups, and n = 8 in the gammapyrone 0.1 + STZ and gammapyrone 0.5 + STZ groups). The animals were acclimated to the experimental room for 30 min, and then each animal was gently placed inside a round arena (d = 100 cm, h = 40 cm) for 10 min. A video tracking device coupled with EthoVision XT 11.0 (Noldus, The Netherlands) was used to record the motility parameters of total distance traveled (cm) and total time spent in the center zone (cm/s).

2.3.4 | Morris water maze test

The Morris water maze test was carried out to assess the spatial learning and memory of the rats 14 days after the STZ injection (n = 8 in the control group, n = 7 in the STZ group, n = 9 in the gammapyrone 0.1 + aCSF and gammapyrone 0.5 + aCSF groups, and n = 8 in the gammapyrone 0.1 + STZ and gammapyrone 0.5 + STZ groups). The apparatus (Ugo Basile, Italy) consisted of a blue circular tank (d = 180 cm) filled with water (23 ± 1°C) to a depth that would cover the plexiglass platform (h = 30 cm, d = 10 cm) for 1–2 cm. Each

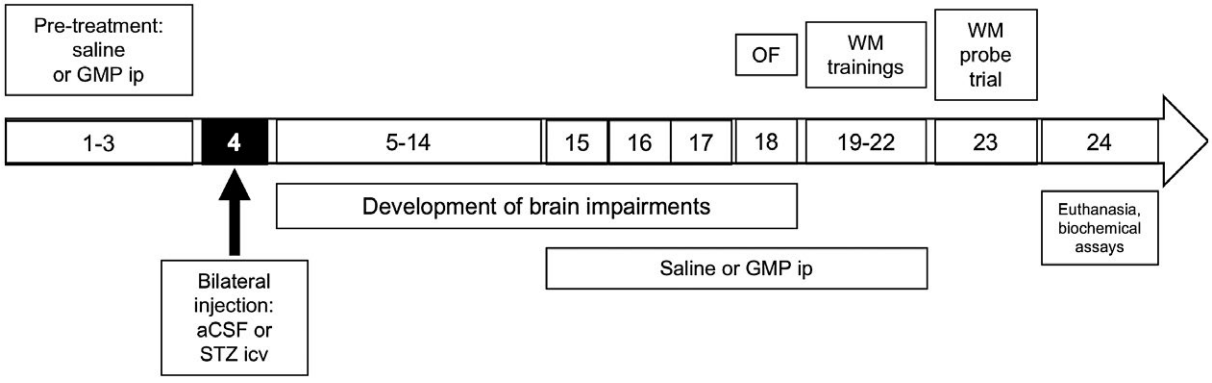

FIGURE 2 Experimental design of the study on gammapyrone (GMP) at doses 0.1 and 0.5 mg/kg. Controls received saline intraperitoneally (ip) and artificial cerebrospinal fluid (aCSF) or streptozocin (STZ); intracerebroventricularly (icv). Behavioral tests included open field (OF) test and the Morris water maze (MWM) test

animal underwent four trials (120 s for each trial) per day for four consecutive days. The animals were trained on experimental days 19–22 to find the hidden platform from different starting points in the pool. Rats were gently put in the water facing the wall of the pool. As soon as the animal found the platform, it was given 15 s to stay on it to learn the location. The intertrial period was 10 min. On experimental day 23, the probe test was carried out. In this case, the platform was taken out of the pool, and each animal had to swim for 120 s in the pool. EthoVision XT 11.0 video tracking software (Noldus, The Netherlands) was used to register the following: (a) rat escape latency, that is, time in seconds for each animal to find the platform after being put in the pool, during trainings and (b) time spent in the target quadrant during the probe trial, and (c) the number of platform zone crossings during the probe trial.

2.4 | Ex vivo assessments

2.4.1 | Immunohistochemical detection

Immunohistochemical analyses were performed to determine the densities of GAD67 (1:500, Santa Cruz Biotechnology, sc-28376, RRID: AB_627650), GFAP (1:1000, Sigma-Aldrich, RRID: AB_477010) and Iba-1 (1:2000, Wako, RRID: AB_839504) in the anterior cingulate cortex and hippocampal *cornu ammonis* (CA1) region. The latter structure was chosen because more pronounced loss of CA1 neurons occurs in AD, correlating with memory impairment (West, Kawas, Martin, & Troncoso, 2006; Zarow et al., 2005). On the next day after the probe trial, rats were deeply anesthetized with ketamine (150 mg/kg) and xylazine (15 mg/kg) and transcardially perfused with ice-cold saline for at least 10 min. After the perfusion, animals were decapitated, and the brains were removed and fixed in 4% paraformaldehyde for 24 hr. After fixation, the brains were placed in 30% sucrose for 48 hr for cryoprotection and subsequently placed in an antifreeze solution.

For each brain, 18 coronal slices per animal (30 μm thick, AP plane: Bregma −2.92 to −3.48 mm in the same animal) were obtained using a cryotome (CM1850, Leica Biosystems, USA). Free floating brain sections were rinsed three times in PBS and 0.1% Triton X-100 solution, incubated in citrate buffer (pH 6.0) at 95°C for 10 min to improve antigen retrieval (for GAD67 and Iba-1), cooled to room temperature (20°C) and blocked with 5% bovine serum albumin solution at room temperature for 1 hr to avoid the formation of background staining. Sections were then stained with respective primary antibody (1:500 for GAD67, 1:1000 for GFAP and 1:2000 for Iba-1). After incubation with the primary antibody, the sections were rinsed in PBS-T 3 times and transferred to a solution containing the biotinylated mouse immunoglobulins (dilution 1:500) raised against GAD67 and GFAP and incubated for 1.5 hr. The Iba-1 sections were incubated with goat anti-rabbit immunoglobulins conjugated with horseradish peroxidase (1:2000) for 2 hr. After incubation with the secondary antibody, the GAD67 and GFAP sections were rinsed three times and incubated with mouse ExtrAvidin Peroxidase (1:1000) for 1.5 hr. After rinsing, the sections were incubated with PBS solution containing 2.5% DAB, 0.2% H_2O_2 and 5% nickel ammonium sulfate for 30 s (Iba-1) or 1 min (GAD67 and GFAP). For Iba-1 and SYP1, the sections were also counterstained for 1 min in hematoxylin solution. All stained sections were mounted on slides and coverslipped. Negative control sections were also stained using the same protocol but without the primary antibody. All experiments were done in duplicate.

2.4.2 | Histochemical assessment

For each brain, six coronal slices per animal (30 μm thick, AP plane: Bregma −2.92 to −3.48 mm in the same animal) were obtained. Histochemical detection of AChE-containing nerve axon density in the anterior cingulate cortex and hippocampal CA1 region was performed using a previously described method (Karnovsky & Roots, 1964), which was optimized and described elsewhere (Kadish & Van Groen, 2002). Briefly, brain sections (n = 5 brain samples per group) were rinsed with a 0.1 M maleate buffer (pH 6.0). Subsequently, the sections were incubated with 0.1 M maleate buffer containing 86.5 mM S-acetylthiocholine iodide, 30 mM ethopropazine, 30 mM copper sulfate, and 100 mM sodium citrate and 0.03 mM potassium hexacyanoferrate for 2 hr. Subsequently, the staining was intensified by incubating the sections with 2.5% DAB, 0.2% H_2O_2 and 5% nickel ammonium sulfate for 2 min in 0.05 M Tris buffer (pH 7.6) for 2 min. All experiments were done in duplicate.

2.4.3 | Quantification

The mounted brain sections (24 sections per animal per group) were digitized using a Pannoramic MIDI II Scanner (3DHISTECH, USA) with a 20X lens. The corresponding regions were then selected, and images were captured using Pannoramic Viewer (RRID: SCR_014424, 3DHISTECH, USA). The optical densities of expressed proteins were measured in the anterior cingulate cortex and the *stratum radiatum* of the hippocampal CA1 region. All measurements were made in duplicate. Both immunohistochemical and histochemical data were quantified using an open-source image processing software (Fiji, RRID: SCR_002285, Germany). A region of interest (same size for all samples) was chosen, and an automatic threshold (in arbitrary units) was chosen to detect pixel density. Densitometry was reported as the mean intensity in arbitrary units per studied region of interest.

2.5 | In vitro assays

2.5.1 | Binding to GABA-A receptor

The experiment was accepted in accordance with Eurofins validation Standard Operating Procedure and performed by CEREP (France). Gammapyrone was tested at 1, 10, and 100 μM concentrations and agonist radioligand [^{3}H]muscimol—at a 15 nM concentration for 120 min at room temperature to assay the binding to the GABA-A1

receptor (α1, β2, and γ2) obtained from human recombinant cells (Wang, 2001). Compound binding was detected using scintillation counting and was calculated as percent inhibition of the binding of a radioactively labeled ligand specific for the GABA-A receptor. Experiment was done two times, with each assay conducted in duplicate. Inhibition or stimulation higher than 50% were considered significant.

2.5.2 | Binding to GABA-B receptor

The brains from adult male Wistar rats (180 ± 20 g) were removed, embedded in cryoglue and cut into 10-μm thick adjacent coronal sections (thalamic nuclei, cerebellum and hippocampus) and membranes were prepared as described previously (Bischoff et al., 1999; Dambrova et al., 2008). In brief, membranes were incubated with the GABA-B receptor-selective radioligand [^{3}H]-CGP 54626 (2 nM) and competing drugs (baclofen and gammapyrone) in 200 μL of Krebs-Henseleit (KH) buffer for 90 min at room temperature. Gammapyrone was tested at 1, 10, and 100 μM concentrations. Non-specific binding for each assay was determined in the presence of 10 mM baclofen. The bound and free radioligands were separated by rapid filtration under a vacuum using Millipore GF/C filter paper (Merck Millipore, USA). The filters were washed three times with 0.25 ml of KH buffer. Radioactivity of the samples was measured with a liquid scintillation counter (Wallac MicroBeta TriLux, PerkinElmer, USA). Each experiment was performed twice, and each assay was conducted in duplicate. Significant inhibition or stimulation was considered to be that of 50% or higher.

2.5.3 | Cell culture

Rat PC12 cells (TCC® CRL-721™, USA) were cultured in DMEM, supplemented with 10% horse serum, 5% FBS, 1% L-glutamine (200 mM), 1% of mixture penicillin (100 international units/ml) and streptomycin (100 μg/ml) at 37°C in a CO_2 incubator. Before the experiments, cells were differentiated by culturing in serum-free medium containing 50 ng/ml nerve growth factor for 5 days. Protein concentration was quantified using Bradford colorimetric protein determination at 595 nm (Bradford, 1976).

2.5.4 | Cell viability and toxicity assay

Cell viability was determined by the MTT assay, based on the ability of living cells to metabolize the yellow tetrazolium salt to a blue formazan via mitochondrial succinate dehydrogenase which is a member of mitochondrial electron transfer system complex. Gammapyrone was added at concentrations 1, 10, and 100 μM. Based on the results obtained from the cell viability assay, 1 μM was the concentration of gammapyrone chosen to perform DEHP toxicity tests.

PC12 cells (2.5×10^5 cells/well in a 96-well plate) were incubated at 37°C after pretreatment with gammapyrone (1 μM) for 2 hr and then incubated with DEHP (83 μM) for 24 hr.

A negative control containing only cells was also evaluated. After treatment with gammapyrone, the cells were incubated with 5 mg/ml MTT for 3 hr at 37°C, the medium was carefully removed after the incubation and the formazan crystals were dissolved in 150 μL dimethyl sulfoxide. Absorbance of formazan reduction product was measured by spectrophotometry at 570 nm using an ELx800™ microplate reader (BioTek Instruments, USA). The results were expressed as the percentage of MTT reduction relative to the absorbance measured from negative control cells. All assays were performed in triplicate.

2.5.5 | Determination of reactive oxygen species (ROS)

To estimate the levels of endogenous ROS formation in control and experimental cells, the nonfluorescent probe DCF-DA, which penetrates into the intracellular matrix of cells and is oxidized through by peroxides in the presence of ROS to form fluorescent 2,7-dichlorofluorescein (Chen, Zhong, Xu, Chen, & Wang, 2010), was used. PC12 cells were seeded on 24-well culture plates (Polylabo, France) at 10^5 cells/well and incubated for 24 hr. Then, the cells were incubated with DEHP alone or combined to gammapyrone (1 μM) for 24 hr at 37°C. After treatment, cells were incubated with 20 μM DCF-DA for 30 min at 37°C and washed twice with PBS to remove the excess probe. The intracellular production of ROS was measured by fluorometric detection of 2,7-dichlorofluorescein oxidation on a fluorimeter (FL 800, BioTek Instruments, USA) with an excitation wavelength of 485 nm and emission wavelength of 522 nm.

2.5.6 | Measurement of mitochondrial membrane potential (MMP)

Changes in MMP were determined by the mitochondrial-specific incorporation of a cationic fluorescent dye Rhodamine-123 (Rh-123) (Debbasch et al., 2001). The cells were seeded in 96-well culture plates and were treated with DEHP alone or combined with gammapyrone (1 μM) for 24 hr. Then, cells were rinsed with PBS, and 100 μL of Rh-123 (1 μM) in PBS was added on the plates. Cells were incubated (37°C, 5% CO_2) for 15 min. Next, the PBS solution containing Rh-123 that was not taken up by the cells was washed and replaced by fresh PBS, and fluorometric detection was done. The results were expressed as the intracellular Rh-123 uptake in arbitrary units. All assays were performed in triplicate.

2.5.7 | Preparation of mitoplasts

PC12 cells were collected by trypsinization, pelleted by centrifugation at 500 ×*g* and resuspended in PBS (pH 7.4). The cell suspension was exposed to 2 mg digitonin/mg cellular proteins for10 min on ice. The mitoplast fraction, obtained by digitonin cell disruption, was pelleted at 14,000 ×*g* and resuspended in PBS (Signorile et al., 2014).

2.5.8 | Enzymatic spectrophotometric assay of mitochondrial complexes

Mitoplasts were exposed to ultrasound energy for 15 s at 0°C. The reduced nicotinamide adenine dinucleotide (NADH):ubiquinone oxidoreductase (complex I) activity was measured by quantifying the oxidation of 100 μM NADH at 340–425 nm ($\Delta\varepsilon$ = 6.81 mM^{-1} cm^{-1}) by 50 μg of mitoplast proteins in 40 mM potassium phosphate buffer (pH 7.4) containing 5 mM $MgCl_2$, 3 mM KCN, 1 μg/ml antimycin, and 200 μM decylubiquinone The activity was corrected for the residual activity measured in the presence of 1 μg/ml rotenone (Piccoli et al., 2006). Succinate-cytochrome c oxidoreductase (complexes II+III) activity was measured at 550–540 nm ($\Delta\varepsilon$ = 19.1 $mM+^{-1}$ cm^{-1}) as the initial rate of cytochrome c reduction. Proteins (100 μg/ml) were incubated for 10 min in the assay buffer (25 mM potassium phosphate, pH 7.2, 5 mM $MgCl_2$) in the presence of 20 mM succinate, 3 μg/ml rotenone, 2 mM KCN and 65 mM decylubiquinone. The reaction, started by the addition of 20 μM cytochrome c, was corrected by the residual activity measured in the presence of 2 μg/ml antimycin A. Cytochrome c oxidase (complex IV) activity was measured by quantifying the oxidation of 10 μM ferrocytochrome c at 550–540 nm ($\Delta\varepsilon$ = 19.1 mM^{-1} cm^{-1}). Enzymatic activity was measured in 10 mM PBS using 30 μg mitoplast proteins (Cooperstein & Lazarow, 1951).

2.5.9 | Measurement of mitochondrial ATP production rate

The rate of ATP production by oxidative phosphorylation was determined in digitonin-permeabilized cells, essentially as described elsewhere (Valenti et al., 2013). Briefly, aliquots of trypsinized fibroblasts washed with PBS were suspended in 1 ml of medium containing 210 mM mannitol, 70 mM sucrose, 20 mM Tris/HCl, 5 mM KH_2PO_4/K_2HPO_4 (pH 7.4), 3 mM $MgCl_2$ in the presence of the ATP detecting system (ATP-ds). The ATP-ds consisted of 2.5 mM glucose, two units hexokinase, one unit glucose 6-phosphate dehydrogenase (G6P-DH) and 0.25 mM nicotinamide adenine dinucleotide phosphate ($NADP^+$), with 3 μM rotenone as toxin and 5 mM succinate as energy substrate, as well as 10 μM diadenosinepentaphosphate as the adenylate kinase inhibitor (Lienhard & Secemski, 1973).

After 5 min of incubation with digitonin (30 μg/10^6 cells) at 37°C, the reduction of $NADP^+$ in the extramitochondrial phase, which reveals adenosine triphosphate (ATP) formation from externally added adenosine diphosphate (ADP, 0.5 mM), was determined as the increase in absorbance at 340 nm. Care was taken to use enough hexokinase/G6P-DH coupled enzymes to ensure a nonlimiting ADP-regenerating system for the measurement of ATP production. The rate of ATP production by Complex V was corrected for the residual ATP production measured in the presence of 2 μg/mg protein oligomycin.

2.5.10 | Protein extraction and Western blot analysis for apoptosis proteins

After the treatment schedule, PC12 cells (1 × 10^5) in 6-well plates were harvested, washed with PBS, and lysed in 100 μL lysis buffer (0.5 M HEPES containing 0.5% Nonidet-P40, 1 mM PMSF, 1 mg/ml aprotinin, 2 mg/ml leupeptin, pH 7.4) and incubated 20 min on ice before centrifugation. Protein concentrations were determined in cell lysates using the Protein BioRad assay.

Equal amounts of proteins (30 μg) were separated on 12% SDS–polyacrylamide gel electrophoresis and subsequently blotted onto PVDF membranes (Millipore, USA). After blocking for 1 hr in TBS containing 5% nonfat dry milk at 25°C, the blots were probed overnight with the following primary antibodies: Bax (1:500, Santa Cruz Biotechnology, AB_626729), Bcl2 (1:500, Santa Cruz Biotechnology, AB_626736), p53 (1:2000, Cell Signaling Technology, AB_331741), caspase 3 (1:500, Santa Cruz Biotechnology, AB_626803), and β-actin overnight at 4°C. The blots were then washed and incubated for 1 hr with the corresponding secondary antibodies: horseradish peroxidase-conjugated anti-mouse or anti-rabbit IgG (both 1:3000). Protein bands were visualized by enhanced chemiluminescence using ECL-kit (GenScript, USA). Proteins levels were then determined by computer-assisted densitometric analysis using GS-800 densitometer (BioRad, USA). All assays were performed in duplicate.

2.6 | Statistical analysis

GraphPad Prism® software (www.graphpad.com, RRID: SCR_002798) was used to conduct the statistical analysis. All data are presented as the mean ± standard deviation (S.D.) values. All data were subjected to the Kolmogorov–Smirnov test for normality and an equal variance test. The Morris water maze training data were analyzed using two-way analysis of variance (ANOVA) with repeated measures to account for inter-group variations (with group and training day as factors) and were followed by Holm-Sidak's multiple comparisons test. Data from the Morris water maze trainings were examined for outliers (>2 standard deviations of the mean); no values that met this criterion were found. The Morris water maze probe trial and open field data, as well as the quantitative immunohistochemical and histochemical data, were analyzed using one-way ANOVA followed by Holm-Sidak's multiple comparisons test. In vitro data (in PC12 cells) were analyzed using one-way ANOVA followed by Tukey's multiple comparisons test. Statistical significance was set at $p < 0.05$.

3 | RESULTS

3.1 | Influence of gammapyrone on rat behavior

3.1.1 | Gammapyrone attenuated STZ-induced spatial learning and memory impairments

Morris water maze test parameters of rats are shown in Figure 3. Differences in groups ($F_{5,43}$ = 7.7, $p < 0.001$), training days ($F_{3,129}$ = 163.1, $p < 0.001$) and between groups and days ($F_{15,129}$ = 2.7, $p = 0.0012$) were observed. Figure 3a shows rat performance during consecutive Morris water maze training days. Administration of STZ resulted in significantly extended latency to reach the escape platform compared to controls on training day 2 ($p = 0.004$), day 3 ($p < 0.001$) and day 4 ($p < 0.001$). STZ rats treated with

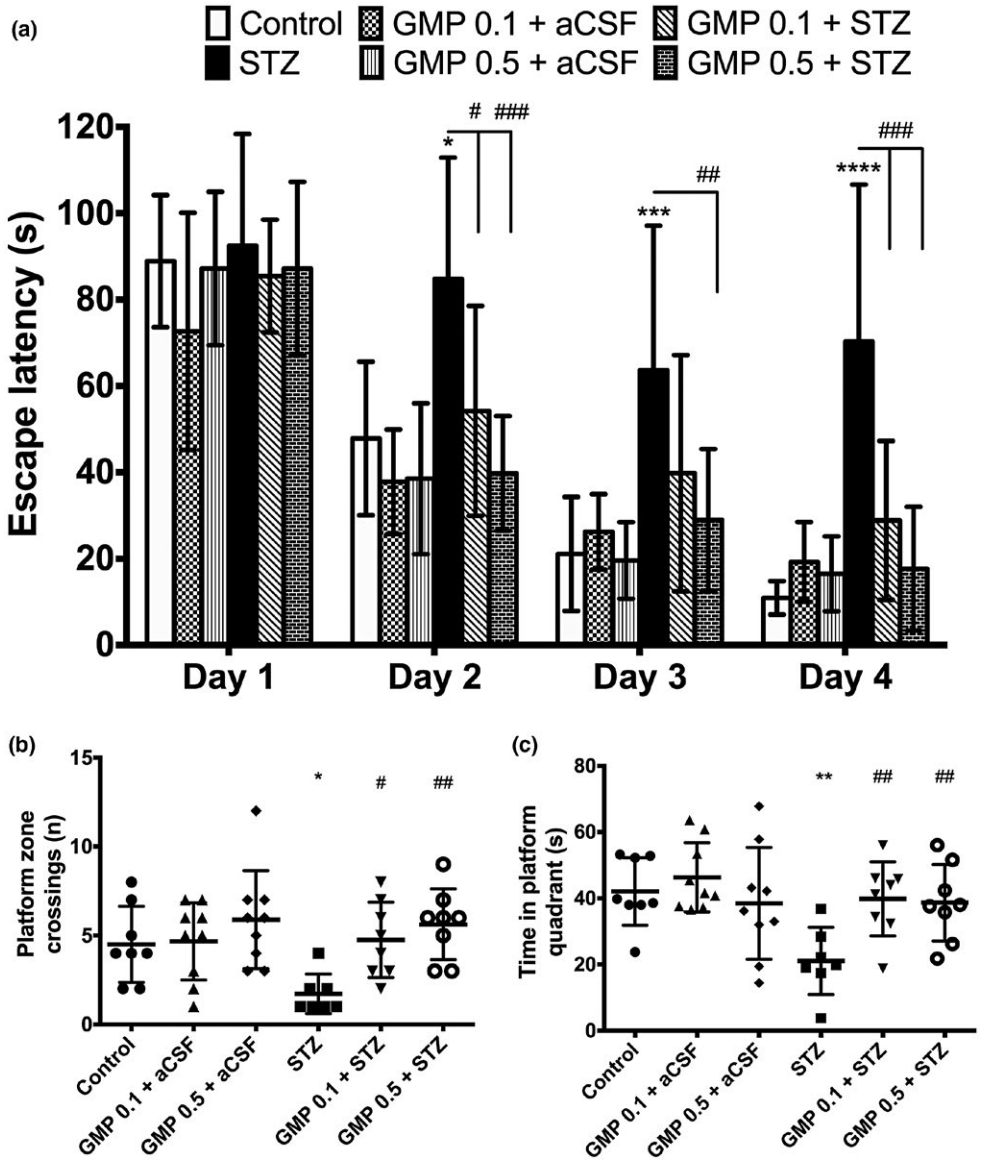

FIGURE 3 Influence of gammapyrone (GMP) on rat performance in the Morris water maze test trainings (a) and in the probe trial (b, c) in streptozocin (STZ)-treated rats. Controls received aCSF intracerebroventricularly (icv) and saline intraperitoneally. The data are shown as mean values ± S.D. Two-way repeated measure ANOVA followed by Holm-Sidak's multiple comparisons test. *$p < 0.05$, **$p < 0.01$, ***$p < 0.001$ and ****$p < 0.0001$ versus Control; #$p < 0.05$, ##$p < 0.01$ and ###$p < 0.001$ versus STZ

gammapyrone in dose 0.1 mg/kg demonstrated significantly shorter escape latency than STZ rats on training day 2 ($p = 0.03$) and day 4 ($p < 0.001$). Treatment with 0.5 mg/kg gammapyrone also resulted in significantly shorter escape latency of STZ rats versus STZ group on training day 2 ($p < 0.001$), day 3 ($p = 0.009$) and day 4 ($p < 0.001$). Differences between groups were discovered also in the probe trial parameters: platform crossings ($F_{5,43} = 3.6$, $p = 0.009$, Figure 3b) and time spent in the platform quadrant ($F_{5,43} = 3.8$, $p = 0.006$, Figure 3c). Rats treated with STZ crossed the platform zone less ($p = 0.02$) and spent markedly less time in the platform quadrant ($p = 0.02$) than the controls. STZ animals treated with gammapyrone at 0.1 mg/kg demonstrated more platform crossings ($p = 0.009$) as well as longer time spent in the target quadrant ($p = 0.005$) in comparison to STZ group rats. STZ animals treated with gammapyrone at 0.5 mg/kg also showed more platform crossings ($p = 0.001$) and spent longer time in the target quadrant ($p = 0.007$) compared to the STZ group.

3.1.2 | Gammapyrone did not alter rat locomotor activity

No significant differences were observed between groups in the total distance traveled ($F_{5,43} = 0.9$, $p = 0.5$) and time spent in the center zone ($F_{5,43} = 1.2$, $p = 0.3$) (data not shown). For the total distance traveled, the mean values were as follows: control 447.4 cm; gammapyrone 0.1 + aCSF: 513.6 cm; gammapyrone 0.5 + aCSF: 414.3 cm; STZ: 376.9 cm; gammapyrone 0.1 + STZ: 638.5 cm; gammapyrone 0.5 + STZ: 467.4 cm. For the time spent in the center zone, the mean values were as follows: control 59.3 s; gammapyrone

0. 1 + aCSF: 71.6 s; gammapyrone 0.5 + aCSF: 65.7 s; STZ: 68.4 s; gammapyrone 0.1 + STZ: 106 s; gammapyrone 0.5 + STZ: 59.6 s.

3.2 | Influence of gammapyrone on protein expression

3.2.1 | Gammapyrone prevented STZ-induced astrocytic activation

Significant differences in GFAP density were found between groups in the cortex ($F_{5,18} = 17.1$, $p < 0.0001$) and in the hippocampus ($F_{5,18} = 6.6$, $p = 0.0012$). Compared to the controls, STZ induced a sharp, almost twofold increase in GFAP density in the cortex ($p < 0.0001$, Figure 4b) and in the hippocampus ($p = 0.0014$, Figure 4d). A significantly lower cortical GFAP density was observed in STZ-injected rats treated with gammapyrone at 0.1 ($p < 0.0001$) and 0.5 mg/kg ($p = 0.0004$) compared to the STZ-treated rats. Treatment with gammapyrone at both doses also significantly reversed STZ-increased GFAP density in the hippocampus ($p < 0.01$).

Neither of the gammapyrone treatments per se influenced cortical or hippocampal GFAP densities.

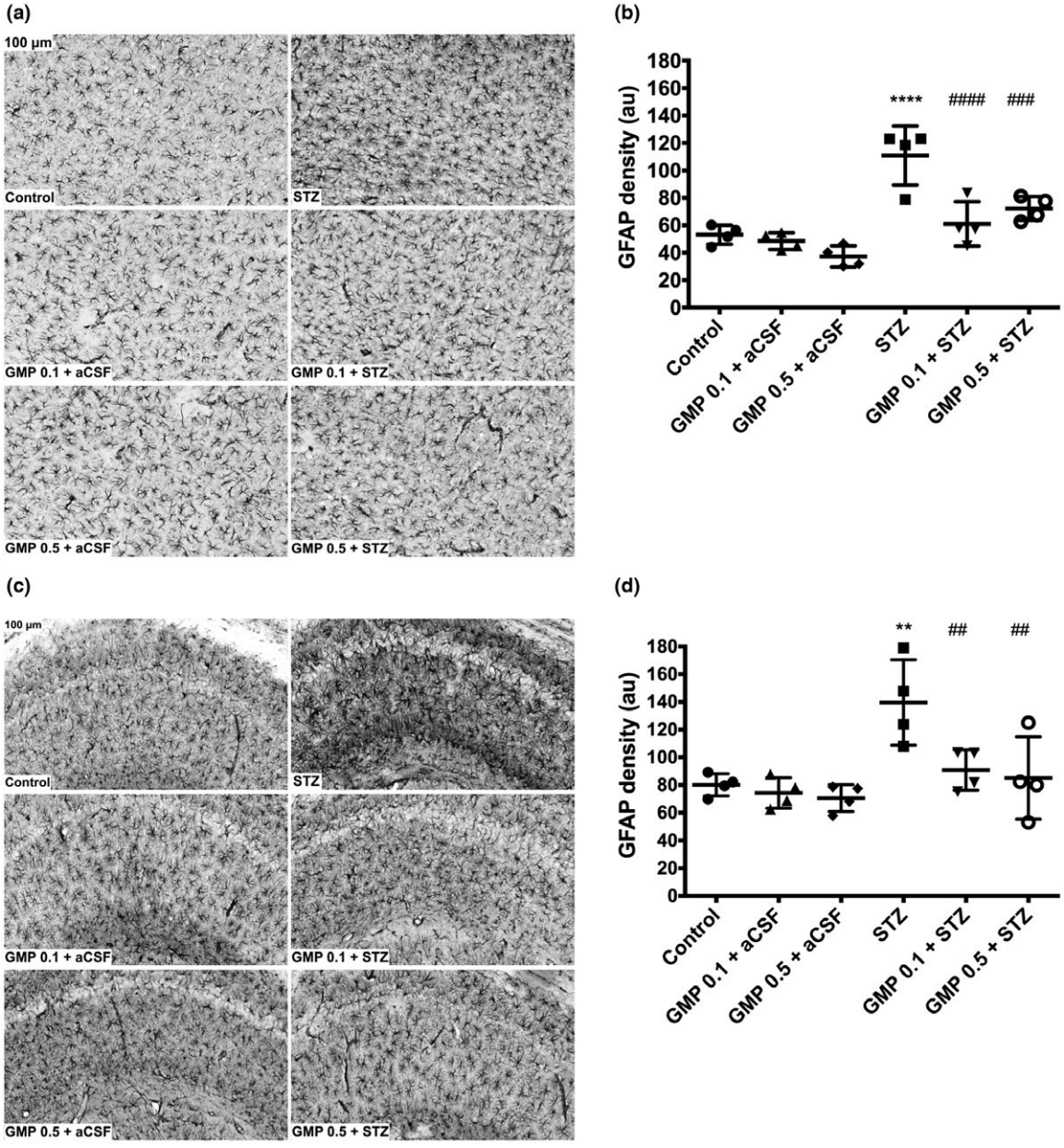

FIGURE 4 Influence of gammapyrone (GMP) on rat glial fibrillary acidic protein (GFAP) expression in streptozocin (STZ)-treated rats. Representative photomicrographs show GFAP-positive astrocytes in the rat anterior cingulate cortex (a) and hippocampal CA1 (c) at 200× magnification. Bar graphs demonstrate cortical (b) and hippocampal (d) density measurements reported as arbitrary units (au). The data are shown as mean values ± S.D. One-way ANOVA followed by Holm-Sidak's multiple comparisons test. $^{**}p < 0.01$ and $^{****}p < 0.0001$ versus Control; $\#\#p < 0.01$, $\#\#\#p < 0.001$ and $\#\#\#\#p < 0.0001$ versus STZ

3.2.2 | Gammapyrone prevented STZ-induced microglial activation

Significant differences in Iba-1 density were found between groups in the cortex ($F_{5,18} = 7.5$, $p = 0.0006$) and in the hippocampus ($F_{5,18} = 12.0$, $p < 0.0001$). STZ-injected animals demonstrated significant increase in Iba-1 density in the cortex ($p = 0.0005$, Figure 5b) and in the hippocampus ($p = 0.0001$, Figure 5d). Cortical Iba-1 density was significantly reduced in STZ-injected rats treated with gammapyrone at 0.1 ($p = 0.012$) and 0.5 mg/kg ($p = 0.008$) compared to the STZ-treated rats. Treatment with gammapyrone at both doses also significantly reversed STZ-increased Iba-1 density in the hippocampus ($p < 0.001$).

Neither of the gammapyrone treatments per se influenced cortical or hippocampal Iba-1 density.

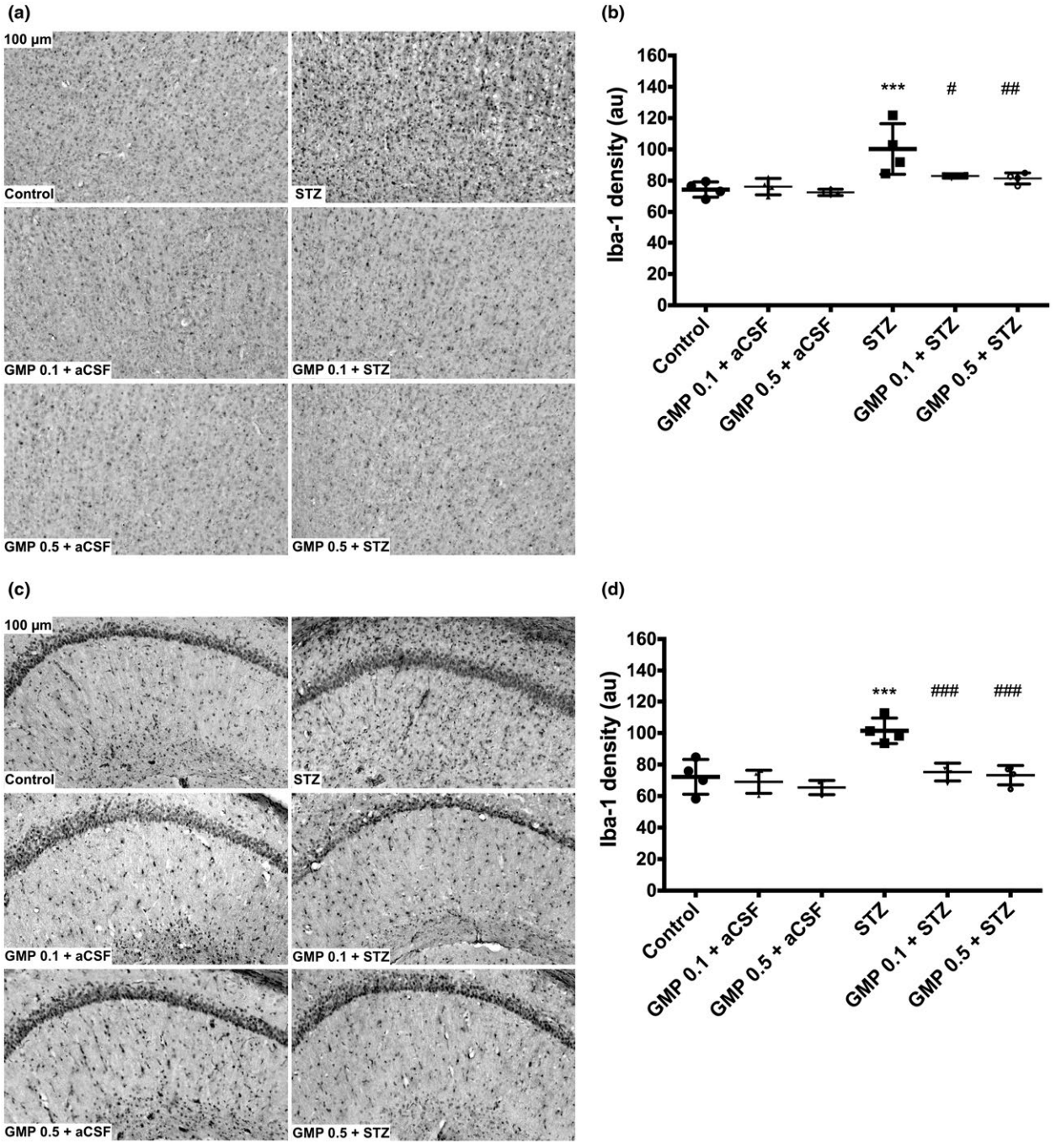

FIGURE 5 Influence of gammapyrone (GMP) on rat Iba-1-positive-cells in streptozocin (STZ)-treated rats. Representative photomicrographs show Iba-1-positive cells in the rat anterior cingulate cortex (a) and hippocampal CA1 (c) at 200× magnification. Bar graphs demonstrate cortical (b) and hippocampal (d) density measurements reported as arbitrary units (au). The data are shown as mean values ± S.D. One-way ANOVA followed by Holm-Sidak's multiple comparisons test. ***$p < 0.001$ versus Control; #$p < 0.05$, ##$p < 0.01$ and ###$p < 0.001$ versus STZ

3.2.3 | Gammapyrone alleviated STZ-induced decrease in GAD67 density

Significant differences in GAD67 density between groups were detected in the cortex ($F_{5,18} = 6.4$, $p = 0.0014$) and in the hippocampus ($F_{5,18} = 4.4$, $p = 0.0081$). Injection of STZ caused a significant decrease in GAD67 density in the cortex ($p = 0.0098$, Figure 6b) and hippocampus ($p = 0.0072$, Figure 6d) in comparison to the controls. STZ rats treated with gammapyrone at 0.1 mg/kg showed significantly higher GAD67 density in the cortex ($p = 0.0024$, Figure 6b) and in the hippocampus ($p = 0.0165$, Figure 6d) compared to STZ group animals. Higher dose of gammapyrone, 0.5 mg/kg,

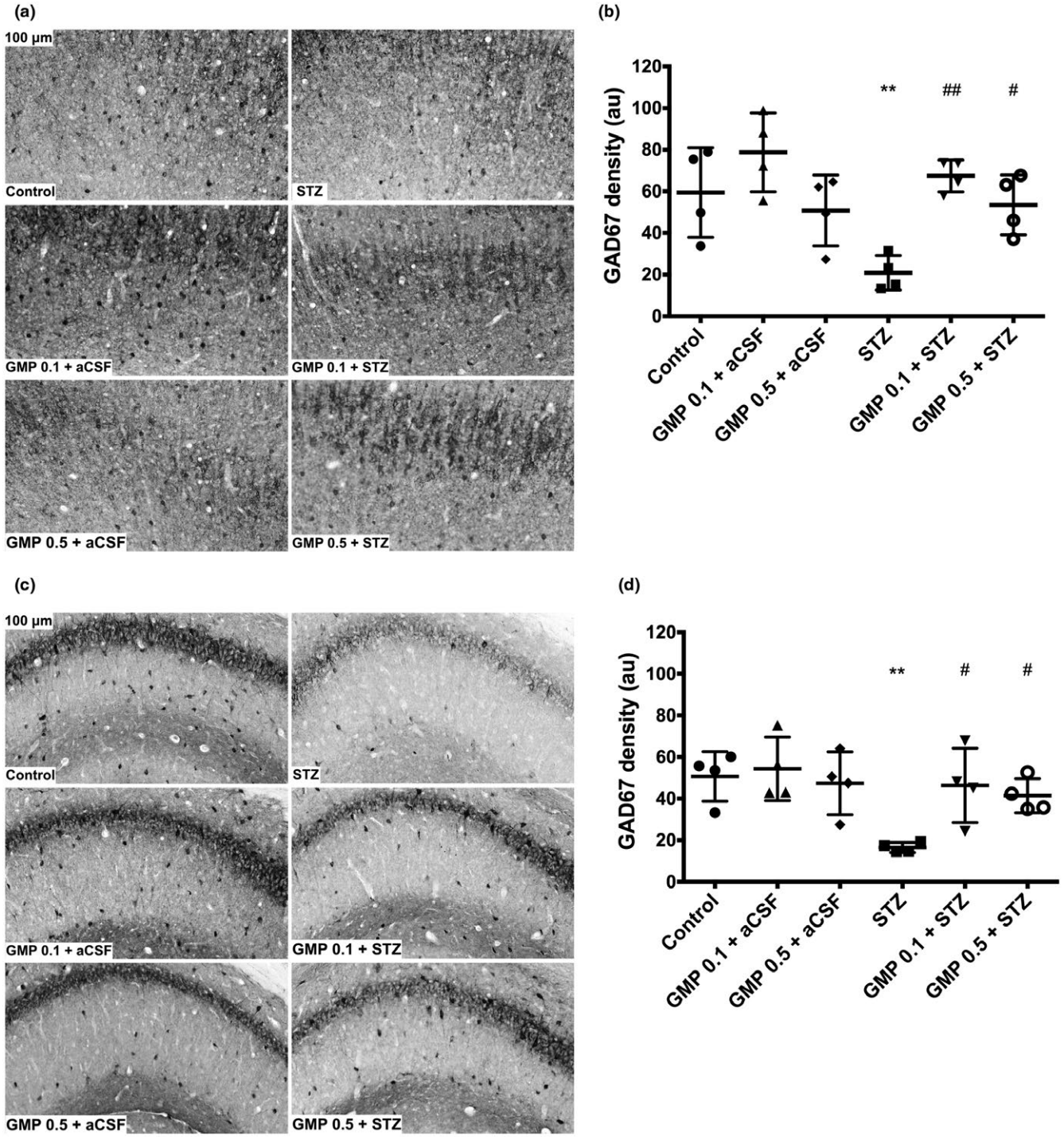

FIGURE 6 Influence of gammapyrone (GMP) on rat glutamate decarboxylase 67 (GAD67) expression in streptozocin (STZ)-treated rats. Representative photomicrographs show GAD67-positive neurons in the rat anterior cingulate cortex (a) and hippocampal CA1 (c) at 200× magnification. Bar graphs demonstrate cortical (b) and hippocampal (d) density measurements reported as arbitrary units (au). The data are shown as mean values ± S.D. One-way ANOVA followed by Holm-Sidak's multiple comparisons test. $^{**}p < 0.01$ and versus Control; $\#p < 0.05$ and $\#\#p < 0.01$ versus STZ

also significantly increased GAD67 density of STZ rats in the cortex ($p = 0.0242$) and in the hippocampus ($p = 0.0398$) compared to the STZ group.

3.2.4 | Gammapyrone reduced the STZ-induced increase in AChE density

Cortical nerve axon density of AChE was significantly different between groups ($F_{5,18} = 4.6$, $p = 0.0004$, Figure 7b), as well as hippocampal ($F_{5,18} = 8.0$, $p = 0.0005$, Figure 7d). Administration of STZ resulted in a significant increase in AChE density in the rat cortex ($p = 0.0188$, Figure 7b) and hippocampus ($p = 0.0018$, Figure 7d) compared to controls. Gammapyrone 0.1 mg/kg significantly reduced the elevated AChE density induced by STZ in the cortex ($p = 0.0003$) and hippocampus ($p = 0.0002$) and at 0.5 mg/kg also ($p = 0.0001$ in the cortex and $p = 0.0005$ in the hippocampus). Gammapyrone per se at either dose did not influence AChE density in the two structures in comparison to the controls.

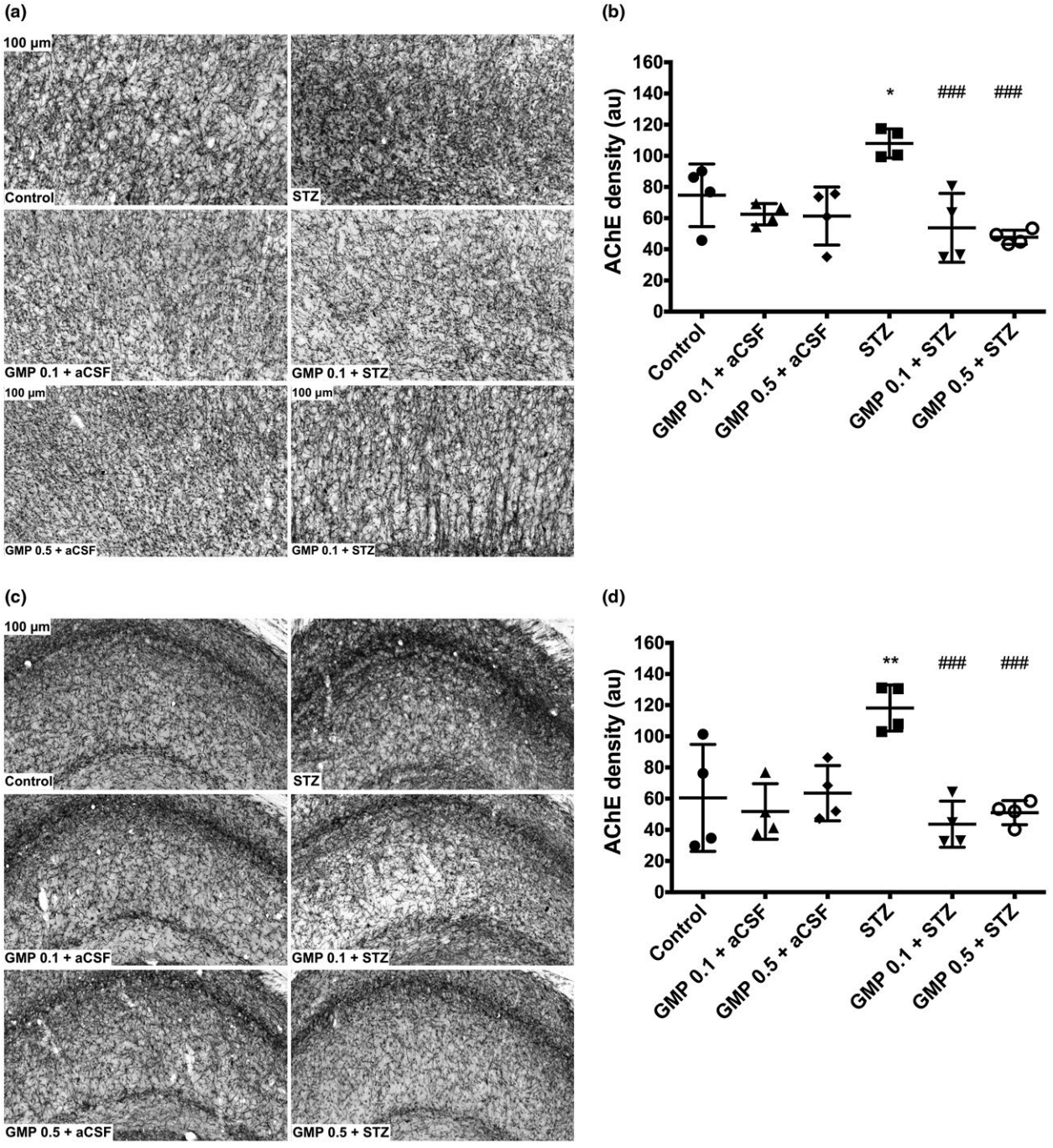

FIGURE 7 Influence of gammapyrone (GMP) on rat AChE density. Representative photomicrographs show AChE-positive nerve axons in the rat anterior cingulate cortex (a) and hippocampal CA1 (c) at 200× magnification. Bar graphs demonstrate cortical (b) and hippocampal (d) density measurements reported as arbitrary units (au). The data are shown as mean values ± S.D. One-way ANOVA followed by Holm-Sidak's multiple comparisons test. *$p < 0.05$ and **$p < 0.01$ versus Control; ###$p < 0.001$ versus STZ

3.3 | Influence of gammapyrone in vitro

3.3.1 | Binding of gammapyrone to GABA-A and GABA-B receptors

Gammapyrone did not show significant inhibition of [3H]muscimol-specific binding. At 100 μM, gammapyrone was able to inhibit [3H] muscimol-specific binding only by 19.3% (data not shown). Even lower inhibition was observed in case of a selective GABA-B receptor antagonist [^{3}H]-CGP 54626-specific binding, at 100 μM reaching only 8.4% (data not shown).

3.3.2 | Influence of gammapyrone on cell viability in PC12 cells

Gammapyrone demonstrated negligible lowering of cell viability at 1–10 μM versus basic level (0 μM), but a sharp decrease was observed at 100 μM ($p < 0.001$, Figure 8a). DEHP induced a twofold decrease in cell viability compared to control ($p < 0.001$, Figure 8b). At nontoxic concentration of 1 μM gammapyrone was capable to significantly improve the viability of DEHP-treated cells ($p < 0.05$, Figure 8b).

3.3.3 | Influence of gammapyrone on ROS production, mitochondrial membrane potential, and the activity of mitochondrial complexes in PC12 cells

In PC12 cells, treatment with DEHP resulted in significantly increased 2,7-dichlorofluorescein oxidation ($p < 0.001$, Figure 9a) and decreased uptake of Rh-123 compared to control ($p < 0.001$, Figure 9b). DEHP also decreased the activity of all mitochondrial complexes (Figure 10a–d): complex I ($p < 0.001$), complex II+III ($p < 0.001$), complex IV ($p < 0.01$) and complex V ($p < 0.01$). In DEHP-treated cells, gammapyrone at 1 μM showed significantly lower fluorescence ($p < 0.001$, Figure 9a), an increase in Rh-123 uptake ($p < 0.001$, Figure 9b), as well as significantly higher activities of all mitochondrial complexes ($p < 0.05$, Figure 10a–c, $p < 0.01$, Figure 10d) compared to the DEHP-treated cells. Gammapyrone per se demonstrated lower values of Rh-123 uptake ($p < 0.01$, Figure 9b) versus control.

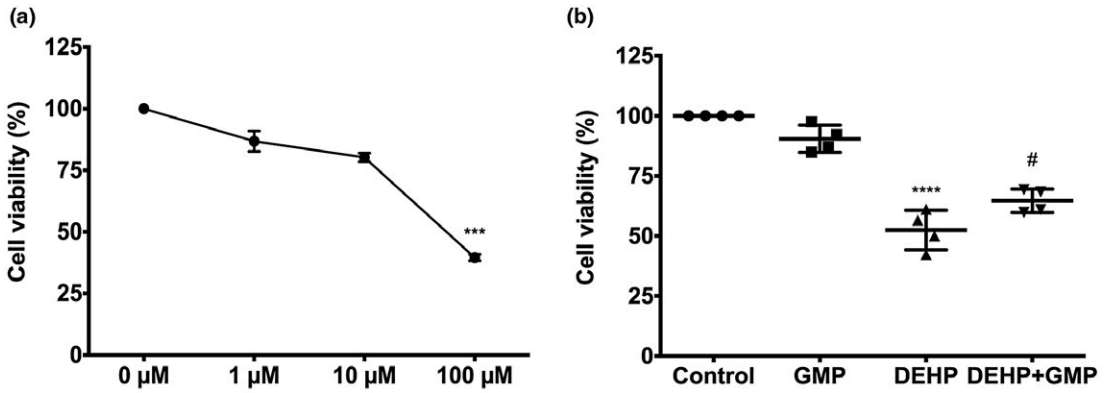

FIGURE 8 Influence of gammapyrone (GMP) on cell viability (a) and, at 1 μM, DEHP-induced cell toxicity (b) in PC12 cells. Non-treated PC12 cells were the control. The data are shown as mean values ± S.D. One-way ANOVA followed by Tukey's multiple comparisons test. *$p < 0.05$ and ***$p < 0.001$ versus Control; #$p < 0.05$ versus DEHP

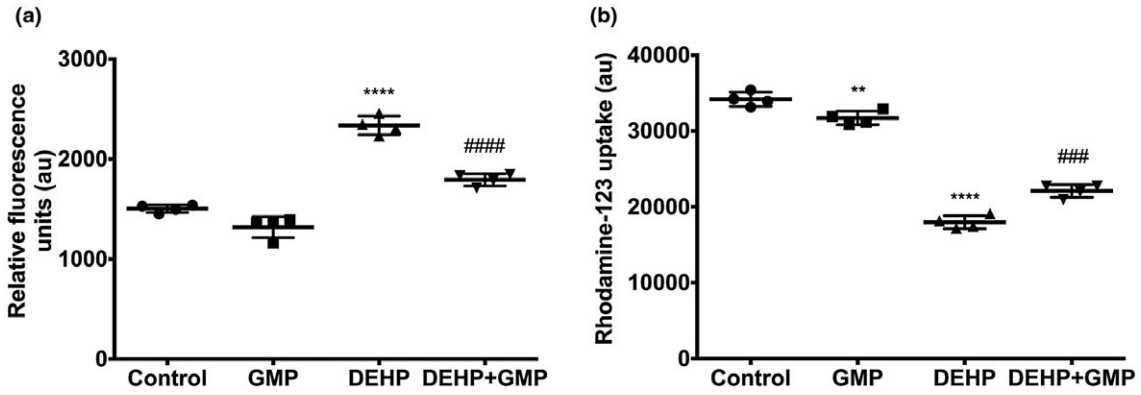

FIGURE 9 Influence of gammapyrone (GMP) at 1 μM on reactive oxygen species production (a) and Rhodamine-123 (Rh-123) uptake (b) against DEHP-induced toxicity in PC12 cells reported as arbitrary units (au). The data are shown as mean values ± S.D. One-way ANOVA followed by Tukey's multiple comparisons test. **$p < 0.01$ and ***$p < 0.001$ versus Control; ###$p < 0.001$ versus DEHP

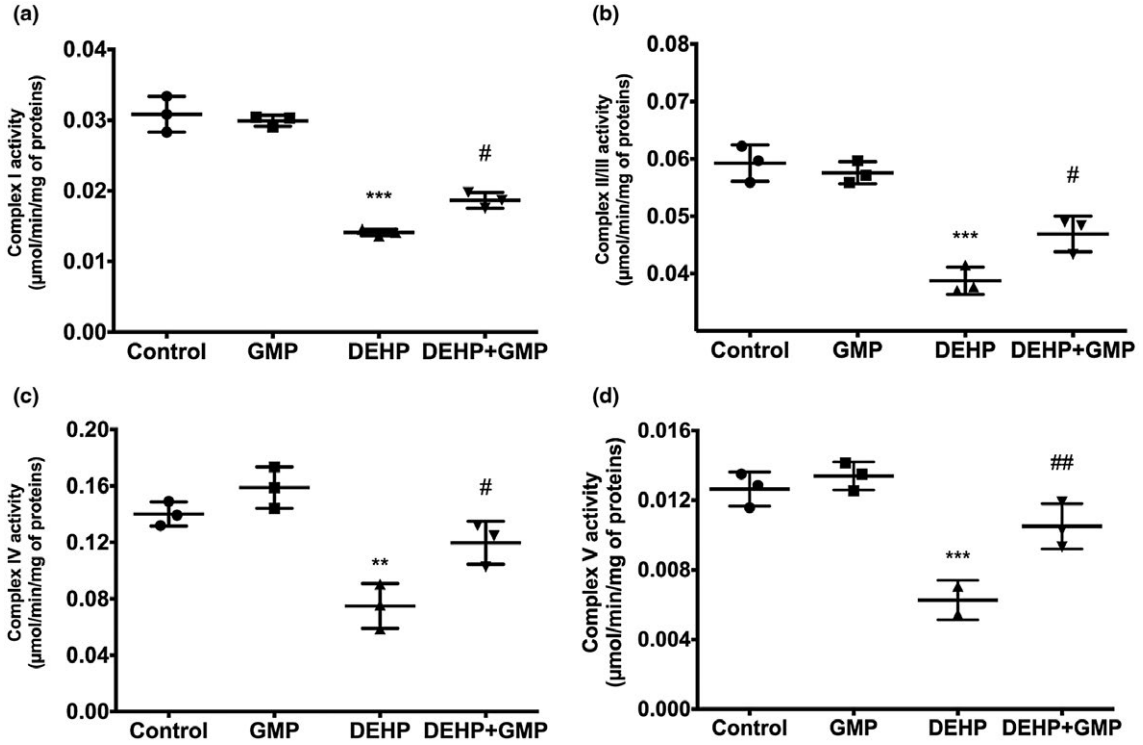

FIGURE 10 Influence of gammapyrone (GMP) at 1 µM on the activity of mitochondrial complexes I (a), complex II/III (b), complex IV (c), and complex V (d) against DEHP-induced toxicity in PC12 cells. The data are shown as mean values ± S.D. One-way ANOVA followed by Tukey's multiple comparisons test. $^{**}p < 0.01$ and $^{****}p < 0.0001$ versus Control; $\#p < 0.05$ versus DEHP

3.3.4 | Influence of gammapyrone on apoptosis markers

Western blot data demonstrated that DEHP induced a significant increase in the density of the apoptosis marker Bax ($p < 0.001$, Figure 11b), significantly reduced the density of Bcl2 ($p < 0.001$, Figure 11a,c) and produced a sharp increase in caspase 3 and p53 density ($p < 0.001$, Figure 11c, f, g, respectively). Gammapyrone was able to significantly reduce the DEHP-induced increase in the density of Bax ($p < 0.01$, Figure 11a, b), caspase 3 and p53 ($p < 0.001$, Figure 11c, e, f, and g, respectively), but did not influence Bcl2 density (Figure 11a, c). Gammapyrone per se did not alter the densities of Bax, Bcl2, and caspase 3, but significantly decreased p53 density compared to the control ($p < 0.01$, Figure 11f, g).

4 | DISCUSSION

4.1 | Gammapyrone effects on the GABAergic system in a male rat AD model

For a long time, the role of GABAergic system in the pathological processes observed in AD was not considered to be important, however, recent reviews demonstrated that the dysfunction of this system plays a major role in the development of neurodegenerative processes (Calvo-Flores Guzmán et al., 2018; Nava-Mesa et al., 2014). It is now well-known that GABA, in addition to glutamate, maintains the excitatory/inhibitory balance, and plays a compensatory role in memory processing (Lanctôt, Herrmaan, Mazzotta, Khan, & Ingber, 2004; Obata, 2013). The importance of GABAergic pathways in remodeling of the AD brain has also been suggested and highlights its role in compensating for the learning and memory impairments in the early stages of AD (Govindpani et al., 2017). Therefore, the GABAergic system is an essential target for the design of novel disease-modifying drugs, although its role in the disease pathogenesis and the cellular changes underlying AD has not been extensively studied (Calvo-Flores Guzmán et al., 2018).

In this context, we examined gammapyrone, a compound containing peptide-like structure ("free" GABA connected to the DHP ring-embedded "crypto" GABA). In the first report on gammapyrone (Misāne et al., 1993), this compound, at a low ip dose of 0.005 mg/kg in naïve rats, was found to enhance memory in the conditioned avoidance response test, and this effect was associated with neuromodulation that manifested as increases in the levels of GABA, noradrenaline, and 5-hydroxyindoleacetic acid in the cortex and hypothalamus.

In the present study, we used a single icv injection of STZ to produce the rapid onset of AD-related symptoms, including neuroinflammation, oxidative stress, glucose hypometabolism, and neurotransmission disruption (Salkovic-Petrisic et al., 2013). These changes result in learning/memory impairments within 1 week after the injection and amyloidosis occurs three weeks after the injection (Paidi et al., 2015). Therefore, this model provides an opportunity to assess novel neuroprotective compounds with a disease-modifying potential and offers better predictive value in translating

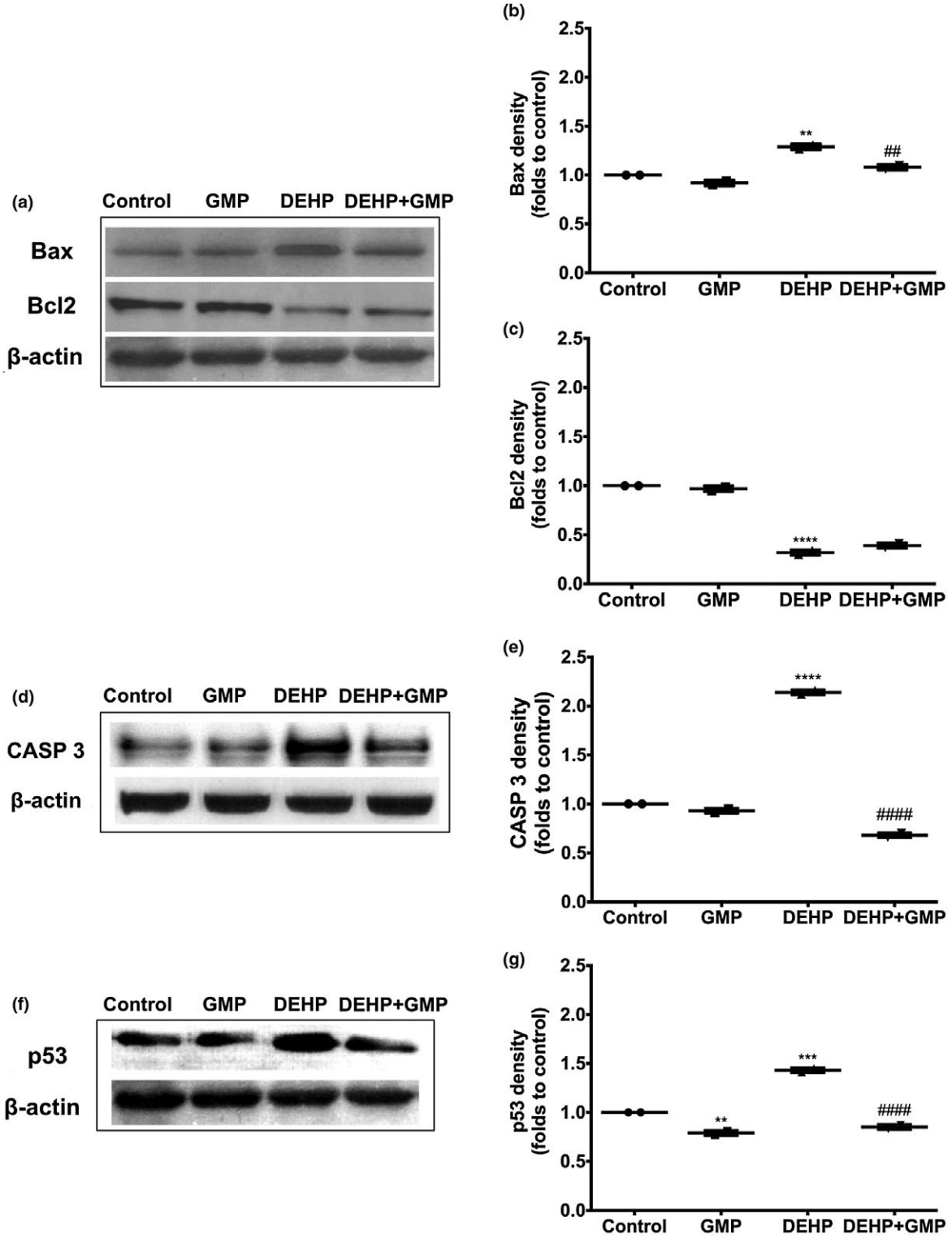

FIGURE 11 Influence of gammapyrone (GMP) at 1 μM on the expression of apoptosis markers Bax and Bcl2 (a), caspase 3 (CASP 3, d) and p53 (f) against di-2-ethylhexyl phthalate (DEHP)-induced toxicity in PC12 cells. Bar graphs demonstrate density measurements of Bax (b), Bcl2 (c), CASP 3 (e), and p53 (g). Graphs demonstrate the ratio for density normalization of the markers to the β-actin. The data are shown as mean values ± S.D. One-way ANOVA followed by Tukey's multiple comparisons test. $^{**}p < 0.01$ and $^{***}p < 0.001$ versus Control; $###p < 0.001$ versus DEHP

the obtained results to humans (Salkovic-Petrisic et al., 2013). One of the limitations of the current study was the use of single sex—male—rats. However, Bao previously reported that the sex differences in STZ rats exist by demonstrating lack of learning and memory impairments, amyloidosis, tau hyperphosphorylation, synaptic, and dendritic plasticity loss in female STZ rats (Bao et al., 2017).

We administered gammapyrone at doses that were comparatively low for DHPs (0.1 and 0.5 mg/kg). In the Morris water maze test, both doses improved spatial learning by significantly shortening the escape latency in STZ-treated animals. Spatial memory was preserved, as demonstrated by a marked increase in platform zone crossings and the time spent in the platform quadrant. However, in the open field, no influence on locomotor activity was observed; the total distance traveled and the time spent in the center zone was not different between animals. Furthermore, gammapyrone reversed the cortical and hippocampal expression of GAD67 in STZ-injected animals to the control levels, indicating the ability to normalize GABA synthesis.

Interestingly, the enhancement of memory and normalization of GAD67 in this study were similar to that observed in our previous investigations of GABA receptor agonists (Pilipenko et al., 2018, 2019). Thus, muscimol (GABA-A GABA site), baclofen (GABA-B), and diazepam (GABA-A benzodiazepine site) were used at very low (subsedative) doses (ranging from 0.01 to 0.05 mg/kg) that were approximately 100 times lower than those inducing memory impairments. These data allowed us to suggest that the actions of low doses of GABA receptor agonists may be mediated by allosteric sites or nonspecific regulatory proteins. We propose that gammapyrone might also act as an allosteric modulator, since in our study, it did not bind to GABA-A and GABA-B receptors. This indicates that specific binding to GABA receptors is not the primary mechanism for the memory enhancing effects of gammapyrone in STZ rats. Nevertheless, we cannot exclude the interaction of gammapyrone with some of the 18 subunits of GABA-A receptor, which are identified in different combinations and exert distinct effects (Enna & McCarson, 2013). Moreover, the binding site for GABA and benzodiazepines has been found on the same protein complex, and a large number of cavities that are capable of binding different substrates and inducing protein conformation changes exist (Sigel & Steinmann, 2012). The complexity might also be attributed to the GABA-B receptor and its subunits (Gassmann & Bettler, 2012; Marshall, Jones, Kaupmann, & Bettler, 1999; O'Leary et al., 2014). In addition, we might speculate that the activity of gammapyrone is also determined by its structural geometry, including the DHP ring, which may act as a molecular chameleon and exert potent actions interacting with different proteins located on ion channels, receptors and enzymes (Triggle, 2003).

Normalizing effects of gammapyrone on the expression of GABA-synthesizing GAD67 led us to suggest that the peptide-like component of its molecule is essential to the mechanism of action of gammapyrone. This might also explain the regulatory effects on the expression of other neuronal (AChE) and glial (GFAP, Iba-1) proteins and mitochondrial processes (see below).

4.2 | Effects of gammapyrone on acetylcholine esterase expression in a male rat AD model

In our study, gammapyrone at both tested doses also normalized AChE expression in AD rat cortex and hippocampus, whereas STZ caused a dramatic increase in AChE expression. It is known that acetylcholine is the key neurotransmitter involved in normal memory functioning (Deiana, Platt, & Riedel, 2011), and that the loss of cholinergic neurons occurs in early AD stages. Moreover, an increase in AChE activity leads to an even greater degradation of acetylcholine (Micheau & Marighetto, 2011). The reversal of AChE overexpression indicates the ability of gammapyrone to regulate cholinergic pathology.

4.3 | Effects of gammapyrone on neuroinflammation in a male rat AD model

Gammapyrone also acts on neuroinflammatory processes, as it was detected by a convincing reduction of STZ-induced astrogliosis and microgliosis in the hippocampus and cortex. Neuroinflammation participates in AD progression via the overactivation of glial cells (Członkowska & Kurkowska-Jastrzębska, 2011; Ransohoff, 2016). Astroglial cells release gliotransmitters that modulate learning and memory as well as maintain synaptic plasticity in the cortex (Ding et al., 2007) and hippocampus (Jourdain et al., 2007). Overactivated astroglial cells, however, release free radicals, proinflammatory cytokines, fatty acid metabolites and prevent neuronal regulatory functioning, thereby inducing learning and memory deficits (Liu & Hong, 2003). Microglia also plays an important role in the maintenance of normal neuronal functioning by continually monitoring their microenvironment and releasing multiple inflammatory mediators (Akiyama et al., 2000). However, when chronically activated, microglia secrete proinflammatory cytokines that further drive a vicious and self-propagating cycle of reactive microgliosis that results in neurodegeneration (Akiyama et al., 2000). Therefore, pharmacotherapeutic approaches that protect against neuroinflammation are currently considered very promising for the treatment of various neurodegenerative diseases (Balducci & Forloni, 2018; González-Reyes, Nava-Mesa, Vargas-Sánchez, Ariza-Salamanca, & Mora-Muñoz, 2017).

4.4 | Effects of gammapyrone on the mitochondrial functioning and apoptosis in PC12 cells

Another target for primary anti-AD strategies is the manipulation of the bioenergetic pathways (Wilkins & Swerdlow, 2016) and/or factors that regulate apoptosis (Shimohama, 2000). AD is strongly associated with mitochondrial dysfunction (Correia et al., 2013). The relationship between mitochondrial impairment and neuroinflammation are still unknown, although it has been reported that these phenomena influence each other (Wilkins & Swerdlow, 2016). Mitochondria are an essential target that regulates protein synthesis and synapse remodeling (Devine & Kittler, 2018). Moreover, neuronal and glial cell death due to apoptosis is a common characteristic found in AD patients. Neuroinflammation and compromised mitochondrial functioning are known to coincide with increased ROS concentrations that induce the overactivation of both astroglial and microglial NO synthases, resulting

in neuronal damage (Morgan & Liu, 2011; Verri et al., 2012). The present results suggest that gammapyrone protects PC12 cells against a variety of detrimental effects caused by DEHP, a toxic agent that induces cell apoptosis and mitochondrial damage (Zeng et al., 2012; Rowdhwal & Chen, 2018). The DEHP model was used to mimic mitochondrial dysfunction (Chen, Yang, Li, Chen, & Xu, 2011). Gammapyrone significantly decreased mitochondrial membrane potential in untreated and in the DEHP-treated cells. Gammapyrone also normalized ROS production, reduced DEHP-induced cell toxicity and restored the activity of all mitochondrial respiratory chain complexes (I-V). Moreover, gammapyrone acted as an anti-apoptotic substance by regulating the expression of proteins involved in cell apoptosis (Bax, caspase 3, and p53). The fact that the toxic effects of DEHP were prevented by 1 μM gammapyrone indicates the potential to restore normal mitochondrial functioning in vitro.

4.5 | General conclusions

The obtained results showed that gammapyrone rescued imbalanced central nervous system functions in the nontransgenic sporadic AD rat model. The effects of gammapyrone treatment manifested as the enhancement of spatial learning/memory, reduction of neuroinflammation, and regulation of neurotransmission. In cell culture, gammapyrone prevented apoptosis, oxidative stress, and mitochondrial dysfunction.

We suggest that the effects of gammapyrone are multifaceted; however, the mechanism of action and the precise target remain to be elucidated. We conclude that gammapyrone molecule and/or its congeners may be considered prototypes for the design of novel disease-modifying agents that target the early stages of sporadic AD.

DECLARATION OF TRANSPARENCY

The authors, reviewers, and editors affirm that in accordance to the policies set by the Journal of Neuroscience Research, this manuscript presents an accurate and transparent account of the study being reported and that all critical details describing the methods and results are present.

ACKNOWLEDGMENTS

We sincerely thank Dr. Edijs Vavers (Latvian Institute of Organic Synthesis) for the help with GABA-B receptor radioligand binding assay and Prof. Gunars Duburs for valuable comments on the manuscript. We also thank Juris Rumaks for technical assistance in the in vivo experiments.

CONFLICT OF INTEREST

We have no conflict of interest to declare.

AUTHOR CONTRIBUTIONS

All authors had full access to all the data in the study and take responsibility for the integrity of the data and the accuracy of the data analysis. Conceptualization, V.C. and V.K.; Methodology, V.P., K.N., I.A., M.S., and A.T.; Investigation, V.P., K.N., I.A., M.S., and A.T.; Formal Analysis, V.P., K.N., I.A., and M.S.; Resources: V.K., B.J., and V.C.; Writing–Original Draft, V.P., K.N., and V.K.; Writing–Review & Editing, V.P., K.N., J.P., V.K., B.J., and V.C.; Visualization, V.P., I.A., and M.S.; Supervision, V.K.; Funding Acquisition, B.J. and V.K.

ORCID

Vladimirs Pilipenko https://orcid.org/0000-0002-7098-7483
Vittorio Calabrese https://orcid.org/0000-0002-0478-985X

REFERENCES

Abolhassani, N., Leon, J., Sheng, Z., Oka, S., Hamasaki, H., Iwaki, T., & Nakabeppu, Y. (2017). Molecular pathophysiology of impaired glucose metabolism, mitochondrial dysfunction, and oxidative DNA damage in Alzheimer's disease brain. *Mechanisms of Ageing and Development*, *161*, 95–104. https://doi.org/10.1016/j.mad.2016.05.005

Akiyama, H., Barger, S., Barnum, S., Bradt, B., Bauer, J., Cole, G. M., … Coray, T. W. (2000). Inflammation and Alzheimer's disease. *Neurobiology of Aging*, *21*, 383–421. https://doi.org/10.1016/S0197-4580(00)00124-X

Balducci, C., & Forloni, G. (2018). Novel targets in Alzheimer's disease: A special focus on microglia. *Pharmacological Research*, *130*, 402–413. https://doi.org/10.1016/j.phrs.2018.01.017

Bao, J., Mahaman, Y. A. R., Liu, R., Wang, J.-Z., Zhang, Z., Zhang, B., & Wang, X. (2017). Sex differences in the cognitive and hippocampal effects of streptozotocin in an animal model of sporadic AD. *Frontiers in Aging Neuroscience*, *9*, 1–12. https://doi.org/10.3389/fnagi.2017.00347

Bischoff, S., Leonhard, S., Reymann, N., Schuler, V., Shigemoto, R., Kaupmann, K., & Bettler, B. (1999). Spatial distribution of GABA(B) R1 receptor mRNA and binding sites in the rat brain. *The Journal of Comparative Neurology*, *412*, 1–16. https://doi.org/10.1002/(SICI)1096-9861(19990913)412:1<1:AID-CNE1>3.0.CO;2-D

Bradford, M. M. (1976). A rapid and sensitive method for the quantitation of microgram quantities of protein utilizing the principle of protein-dye binding. *Analytical Biochemistry*, *72*, 248–254. https://doi.org/10.1016/0003-2697(76)90527-3

Calabrese, V., Santoro, A., Monti, D., Crupi, R., Di Paola, R., Latteri, S., … Franceschi, C. (2018). Aging and Parkinson's disease: Inflammaging, neuroinflammation and biological remodeling as key factors in pathogenesis. *Free Radical Biology and Medicine*, *115*, 80–91. https://doi.org/10.1016/j.freeradbiomed.2017.10.379

Calsolaro, V., & Edison, P. (2016). Neuroinflammation in Alzheimer's disease: Current evidence and future directions. *Alzheimer's & Dementia: The Journal of the Alzheimer's Association*, *12*, 719–732. https://doi.org/10.1016/j.jalz.2016.02.010

Calvo-Flores Guzmán, B., Vinnakota, C., Govindpani, K., Waldvogel, H. J., Faull, R. L. M., & Kwakowsky, A. (2018). The GABAergic system as a therapeutic target for Alzheimer's disease. *Journal of Neurochemistry*, *146*, 649–669. https://doi.org/10.1111/jnc.14345

Chen, T., Yang, W., Li, Y., Chen, X., & Xu, S. (2011). Mono-(2-ethylhexyl) phthalate impairs neurodevelopment: Inhibition of proliferation and promotion of differentiation in PC12 cells. *Toxicology Letters*, *201*, 34–41. https://doi.org/10.1016/j.toxlet.2010.12.002

Chen, X., Zhong, Z., Xu, Z., Chen, L., & Wang, Y. (2010). 2′,7′-Dichlorodihydrofluorescein as a fluorescent probe for reactive oxygen species measurement: Forty years of application and controversy. *Free Radical Research*, *44*, 587–604. https://doi.org/10.3109/10715761003709802

Cooperstein, S., & Lazarow, A. (1951). A microspectrophotometric method for the determination of cytochrome oxidase. *Journal of Biological Chemistry*, *189*(2), 665–670.

Correia, S. C., Perry, G., & Moreira, P. I. (2016). Mitochondrial traffic jams in Alzheimer's disease - pinpointing the roadblocks. *Biochimica et Biophysica Acta (BBA) - Molecular Basis of Disease*, *1862*, 1909–1917. https://doi.org/10.1016/j.bbadis.2016.07.010

Correia, S. C., Santos, R. X., Santos, M. S., Casadesus, G., LaManna, J. C., Perry, G., … Moreira, P. I. (2013). Mitochondrial abnormalities in a streptozotocin-induced rat model of sporadic Alzheimer's disease. *Current Alzheimer Research*, *10*, 406–419. https://doi.org/10.2174/1567205011310040006

Członkowska, A., & Kurkowska-Jastrzębska, I. (2011). Inflammation and gliosis in neurological diseases – clinical implications. *Journal of Neuroimmunology*, *231*, 78–85. https://doi.org/10.1016/j.jneuroim.2010.09.020

Dambrova, M., Zvejniece, L., Liepinsh, E., Cirule, H., Zharkova, O., Veinberg, G., & Kalvinsh, I. (2008). Comparative pharmacological activity of optical isomers of phenibut. *European Journal of Pharmacology*, *583*, 128–134. https://doi.org/10.1016/j.ejphar.2008.01.015

De la Monte, S. M., & Wands, J. R. (2008). Alzheimer's disease is type 3 diabetes—Evidence reviewed. *Journal of Diabetes Science and Technology*, *2*, 1101–1113. https://doi.org/10.1177/193229680800200619

Debbasch, C., Pisella, P. J., De Saint Jean, M., Rat, P., Warnet, J. M., & Baudouin, C. (2001). Mitochondrial activity and glutathione injury in apoptosis induced by unpreserved and preserved β-blockers on chang conjunctival cells. *Investigative Ophthalmology & Visual Science*, *42*, 2525–2533. https://doi.org/10.1117/12.626961

Deiana, S., Platt, B., & Riedel, G. (2011). The cholinergic system and spatial learning. *Behavioral Brain Research*, *221*, 389–411. https://doi.org/10.1016/j.bbr.2010.11.036

Devine, M. J., & Kittler, J. T. (2018). Mitochondria at the neuronal presynapse in health and disease. *Nature Reviews Neuroscience*, *19*, 63–80. https://doi.org/10.1038/nrn.2017.170

Ding, S., Fellin, T., Zhu, Y., Lee, S., Auberson, Y. P., Meaney, D. F., … Haydon, P. G. (2007). Enhanced astrocytic Ca2+ signals contribute to neuronal excitotoxicity after status epilepticus. *Journal of Neuroscience*, *27*, 10674–10684. https://doi.org/10.1523/JNEUROSCI.2001-07.2007

Duran-Aniotz, C., & Hetz, C. (2016). Glucose metabolism: A sweet relief of Alzheimer's disease. *Current Biology*, *26*, R806–R809. https://doi.org/10.1016/j.cub.2016.07.060

Dzirkale, Z., Pupure, J., Rumaks, J., Svirskis, S., Vanina, M., Mezhapuke, R., … Klusa, V. (2011). Comparative study of taurine and tauropyrone: GABA receptor binding, mitochondrial processes and behaviour. *Journal of Pharmacy and Pharmacology*, *63*, 230–237. https://doi.org/10.1111/j.2042-7158.2010.01204.x

Enna, S. J., & McCarson, K. E. (2013). Characterization of GABA receptors. *Current Protocols in Pharmacology*, *1*, 1–20. https://doi.org/10.1002/0471141755.ph0107s63

Gassmann, M., & Bettler, B. (2012). Regulation of neuronal GABAB receptor functions by subunit composition. *Nature Reviews Neuroscience*, *13*, 380–394. https://doi.org/10.1038/nrn3249

González-Reyes, R. E., Nava-Mesa, M. O., Vargas-Sánchez, K., Ariza-Salamanca, D., & Mora-Muñoz, L. (2017). Involvement of Astrocytes in Alzheimer's disease from a neuroinflammatory and oxidative stress perspective. *Frontiers in Molecular Neuroscience*, *10*, 1–20. https://doi.org/10.3389/fnmol.2017.00427

Govindpani, K., Guzmán, B. C. F., Vinnakota, C., Waldvogel, H. J., Faull, R. L., & Kwakowsky, A. (2017). Towards a better understanding of GABAergic remodeling in alzheimer's disease. *International Journal of Molecular Sciences*, *18*, https://doi.org/10.3390/ijms18081813

Grieb, P. (2016). Intracerebroventricular streptozotocin injections as a model of Alzheimer's disease: In search of a relevant mechanism. *Molecular Neurobiology*, *53*, 1741–1752. https://doi.org/10.1007/s12035-015-9132-3

Gross, E. (1977). α, β-Unsaturated and related amino acids in peptides and proteins. *Advances in Experimental Medicine and Biology*, *86B*, 131–153. https://doi.org/10.1007/978-1-4757-9113-6_9

Jourdain, P., Bergersen, L. H., Bhaukaurally, K., Bezzi, P., Santello, M., Domercq, M., … Volterra, A. (2007). Glutamate exocytosis from astrocytes controls synaptic strength. *Nature Neuroscience*, *10*, 331–339. https://doi.org/10.1038/nn1849

Kadish, I., & Van Groen, T. (2002). Low levels of estrogen significantly diminish axonal sprouting after entorhinal cortex lesions in the mouse. *Journal of Neuroscience*, *22*, 4095–4102. https://doi.org/10.1523/JNEUROSCI.22-10-04095.2002

Karnovsky, J. M., & Roots, L. (1964). A "direct-coloring" thiocholine method for cholinesterases. *Journal of Histochemistry and Cytochemistry*, *219–221*, https://doi.org/10.1177/12.3.219

Klusa, V. (2016). Atypical 1,4-dihydropyridine derivatives, an approach to neuroprotection and memory enhancement. *Pharmacological Research*, *113*, 754–759. https://doi.org/10.1016/j.phrs.2016.05.017

Lanctôt, K. L., Herrmaan, N., Mazzotta, P., Khan, L. R., & Ingber, N. (2004). GABAergic function in Alzheimer's disease: Evidence for dysfunction and potential as a therapeutic target for the treatment of behavioral and psychological symptoms of dementia. *Canadian Journal of Psychiatry*, *49*, 439–453. https://doi.org/10.1177/070674370404900705

Lienhard, G. E., & Secemski, I. I. (1973). P1, P5-Di(adenosine-5')pentaphosphate, a potent multisubstrate inhibitor of adenylate kinase. *Journal of Biological Chemistry*, *248*, 1121–1123.

Lithfous, S., Dufour, A., & Després, O. (2013). Spatial navigation in normal aging and the prodromal stage of Alzheimer's disease: Insights from imaging and behavioral studies. *Ageing Research Reviews*, *12*, 201–213. https://doi.org/10.1016/j.arr.2012.04.007

Liu, B., & Hong, J.-S. (2003). Role of microglia in inflammation-mediated neurodegenerative diseases: Mechanisms and strategies for therapeutic intervention. *Journal of Pharmacology and Experimental Therapeutics*, *304*, 1–7. https://doi.org/10.1124/jpet.102.035048

Liu, X., Chen, K., Wu, T., Weidman, D., Lure, F., & Li, J. (2018). Use of multimodality imaging and artificial intelligence for diagnosis and prognosis of early stages of Alzheimer's disease. *Translational Research*, *194*, 56–67. https://doi.org/10.1016/j.trsl.2018.01.001

Liu, X., Jiao, B., & Shen, L. (2018). The epigenetics of Alzheimer's disease: Factors and therapeutic implications. *Frontiers in Genetics*, *9*, 1–10. https://doi.org/10.3389/fgene.2018.00579

Marshall, F. H., Jones, K. A., Kaupmann, K., & Bettler, B. (1999). GABA(B) receptors - The first 7TM heterodimers. *Trends in Pharmacological Sciences*, *20*, 396–399. https://doi.org/10.1016/S0165-6147(99)01383-8

McDade, E., & Bateman, R. J. (2017). Stop Alzheimer's before it starts. *Nature*, *547*, 153. https://doi.org/10.1038/547153a

Micheau, J., & Marighetto, A. (2011). Acetylcholine and memory: A long, complex and chaotic but still living relationship. *Behavioral Brain Research*, *221*, 424–429. https://doi.org/10.1016/j.bbr.2010.11.052

Misāne, I., Cēbers, G., Liepa, I., Dambrova, M., Ģermāne, S., Kluša, V., D … Bisenieks, E. (1993). Cyclic nootropics: similarity and differences in their memory improving action. *Proceedings of the Latvian Academy of Sciences. Section B*, *5*, 81-85

Misane, I., Klusa, V., Dambrova, M., Germane, S., Duburs, G., Bisenieks, E., … Ögren, S. O. (1998). "Atypical" neuromodulatory profile of glutapyrone, a representative of a novel "class" of amino acid-containing dipeptide-mimicking 1,4-dihydropyridine (DHP) compounds: In vitro and in vivo studies. *European Neuropsychopharmacology*, *8*, 329–347. https://doi.org/10.1016/S0924-977X(97)00097-7

Morgan, M. J., & Liu, Z. G. (2011). Crosstalk of reactive oxygen species and NF-κB signaling. *Cell Research*, *21*, 103–115. https://doi.org/10.1038/cr.2010.178

Nava-Mesa, M. O., Jiménez-Díaz, L., Yajeya, J., & Navarro-Lopez, J. D. (2014). GABAergic neurotransmission and new strategies of neuromodulation to compensate synaptic dysfunction in early stages of Alzheimer's disease. *Frontiers in Cellular Neuroscience*, *8*, 167. https://doi.org/10.3389/fncel.2014.00167

O'Leary, O. F., Felice, D., Galimberti, S., Savignac, H. M., Bravo, J. A., Crowley, T., … Cryan, J. F. (2014). GABA $_{B(1)}$ receptor subunit isoforms differentially regulate stress resilience. *Proceedings of the National Academy of Sciences*, *111*, 15232–15237. https://doi.org/10.1073/pnas.1404090111

Obata, K. (2013). Synaptic inhibition and ^|^gamma;-aminobutyric acid in the mammalian central nervous system. *Proceedings of the Japan Academy, Series B*, *89*, 139–156. https://doi.org/10.2183/pjab.89.139

Paidi, R., Nthenge-Ngumbau, D., Singh, R., Kankanala, T., Mehta, H., & Mohanakumar, K. (2015). Mitochondrial deficits accompany cognitive decline following single bilateral intracerebroventricular streptozotocin. *Current Alzheimer Research*, *12*, 785–795. https://doi.org/10.2174/1567205012666150710112618

Paxinos, G., & Watson, C. (2007). *The Rat Brain*. Cambridge, MA: Academic Press.

Pennisi, M., Crupi, R., Di Paola, R., Ontario, M. L., Bella, R., Calabrese, E. J., … Calabrese, V. (2017). Inflammasomes, hormesis, and antioxidants in neuroinflammation: Role of NRLP3 in Alzheimer disease. *Journal of Neuroscience Research*, *95*, 1360–1372. https://doi.org/10.1002/jnr.23986

Piccoli, C., Scacco, S., Bellomo, F., Signorile, A., Iuso, A., Boffoli, D., … Papa, S. (2006). cAMP controls oxygen metabolism in mammalian cells. *FEBS Letters*, *580*, 4539–4543. https://doi.org/10.1016/j.febslet.2006.06.085

Pilipenko, V., Narbute, K., Beitnere, U., Rumaks, J., Pupure, J., Jansone, B., & Klusa, V. (2018). Very low doses of muscimol and baclofen ameliorate cognitive deficits and regulate protein expression in the brain of a rat model of streptozocin-induced Alzheimer's disease. *European Journal of Pharmacology*, *818*, 381–399. https://doi.org/10.1016/j.ejphar.2017.11.012

Pilipenko, V., Narbute, K., Pupure, J., Rumaks, J., Jansone, B., & Klusa, V. (2019). Neuroprotective action of diazepam at very low and moderate doses in Alzheimer's disease model rats. *Neuropharmacology*, *144*, 319–326. https://doi.org/10.1016/j.neuropharm.2018.11.003

Rai, S., Kamat, P. K., Nath, C., & Shukla, R. (2014). Glial activation and post-synaptic neurotoxicity: The key events in Streptozotocin (ICV) induced memory impairment in rats. *Pharmacology, Biochemistry and Behavior*, *117*, 104–117. https://doi.org/10.1016/j.pbb.2013.11.035

Ransohoff, R. M. (2016). How neuroinflammation contributes to neurodegeneration. *Science*, *353*, 777–783. https://doi.org/10.1126/science.aag2590.

Rowdhwal, S. S. S., & Chen, J. (2018). Toxic effects of Di-2-ethylhexyl phthalate: An overview. *BioMed Research International*, *2018*, 1–10. https://doi.org/10.1155/2018/1750368

Salkovic-Petrisic, M., Knezovic, A., Hoyer, S., & Riederer, P. (2013). What have we learned from the streptozotocin-induced animal model of sporadic Alzheimer's disease, about the therapeutic strategies in Alzheimer's research. *Journal of Neural Transmission*, *120*, 233–252. https://doi.org/10.1007/s00702-012-0877-9

Saxena, G., Patro, I. K., & Nath, C. (2011). ICV STZ induced impairment in memory and neuronal mitochondrial function: A protective role of nicotinic receptor. *Behavioral Brain Research*, *224*, 50–57. https://doi.org/10.1016/j.bbr.2011.04.039

Shimohama, S. (2000). Apoptosis in Alzheimer ' s disease—An update. *Apoptosis*, *5*, 9–16. https://doi.org/10.1023/A:1009625323388

Sigel, E., & Steinmann, M. E. (2012). Structure, function, and modulation of GABAA receptors. *Journal of Biological Chemistry*, *287*, 40224–40231. https://doi.org/10.1074/jbc.R112.386664

Signorile, A., Micelli, L., De Rasmo, D., Santeramo, A., Papa, F., Ficarella, R., … Papa, S. (2014). Regulation of the biogenesis of OXPHOS complexes in cell transition from replicating to quiescent state. Involvement of PKA and effect of hydroxytyrosol. *Biochimica et Biophysica Acta (BBA) - Molecular Cell Research*, *1843*, 675–684. https://doi.org/10.1016/j.bbamcr.2013.12.017

Styr, B., & Slutsky, I. (2018). Imbalance between firing homeostasis and synaptic plasticity drives early-phase Alzheimer's disease. *Nature Neuroscience*, *21*, 463–473. https://doi.org/10.1038/s41593-018-0080-x

Tiwari, V., Kuhad, A., Bishnoi, M., & Chopra, K. (2009). Chronic treatment with tocotrienol, an isoform of vitamin E, prevents intracerebroventricular streptozotocin-induced cognitive impairment and oxidative-nitrosative stress in rats. *Pharmacology, Biochemistry and Behavior*, *93*, 183–189. https://doi.org/10.1016/j.pbb.2009.05.009

Triggle, D. J. (2003). 1,4-Dihydropyridines as calcium channel ligands and privileged structures. *Cellular and Molecular Neurobiology*, *23*, 293–303. https://doi.org/10.1023/A:1023632419813

Valenti, D., De Rasmo, D., Signorile, A., Rossi, L., de Bari, L., Scala, I., … Vacca, R. A. (2013). Epigallocatechin-3-gallate prevents oxidative phosphorylation deficit and promotes mitochondrial biogenesis in human cells from subjects with Down's syndrome. *Biochimica et Biophysica Acta (BBA) - Molecular Basis of Disease*, *1832*, 542–552. https://doi.org/10.1016/j.bbadis.2012.12.011

Verri, M., Pastoris, O., Dossena, M., Aquilani, R., Guerriero, F., Cuzzoni, G., … Bongiorno, A. I. (2012). Mitochondrial alterations, oxidative stress and neuroinflammation in Alzheimer's disease. *International Journal of Immunopathology and Pharmacology*, *25*, 345–353. https://doi.org/10.1177/039463201202500204

Wang, X.-K. (2001). Pharmacological study on recombinant human GABA-A receptor complex containing alpha5 (leucine155 to valine) combined with beta3gamma2s subunits. *Acta Pharmacologica Sinica*, *22*, 521–523.

West, M. J., Kawas, C. H., Martin, L. J., & Troncoso, J. C. (2006). The CA1 region of the human hippocampus is a hot spot in Alzheimer's disease. *Annals of the New York Academy of Sciences*, *908*, 255–259. https://doi.org/10.1111/j.1749-6632.2000.tb06652.x

Wilkins, H. M., & Swerdlow, R. H. (2016). Relationships between mitochondria and neuroinflammation: Implications for Alzheimer's disease. *Current Topics in Medicinal Chemistry*, *16*, 849–857. https://doi.org/10.1097/OGX.0000000000000256.Prenatal

Zarow, C., Vinters, H. V., Ellis, W. G., Weiner, M. W., Mungas, D., White, L., & Chui, H. C. (2005). Correlates of hippocampal neuron number in Alzheimer's disease and ischemic vascular dementia. *Annals of Neurology*, *57*, 896–903. https://doi.org/10.1002/ana.20503

Zeng, L., Li, T., Xu, D. C., Liu, J., Mao, G., Cui, M. Z., … Xu, E. (2012). Death receptor 6 induces apoptosis not through type I or type II pathways, but via a unique mitochondria-dependent pathway by interacting with bax protein. *Journal of Biological Chemistry*, *287*, 29125–29133. https://doi.org/10.1074/jbc.M112.362038.

SUPPORTING INFORMATION

Additional supporting information may be found online in the Supporting Information section at the end of the article.

Transparent Science Questionnaire for Authors.

How to cite this article: Pilipenko V, Narbute K, Amara I, et al. GABA-containing compound gammapyrone protects against brain impairments in Alzheimer's disease model male rats and prevents mitochondrial dysfunction in cell culture. *J Neurosci Res*. 2019;97:708–726. https://doi.org/10.1002/jnr.24396